Electronic properties of *Graphene*

Reza Asgari

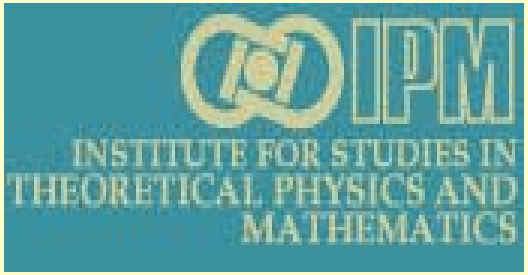

Graphene is the Mother of all Graphitic forms

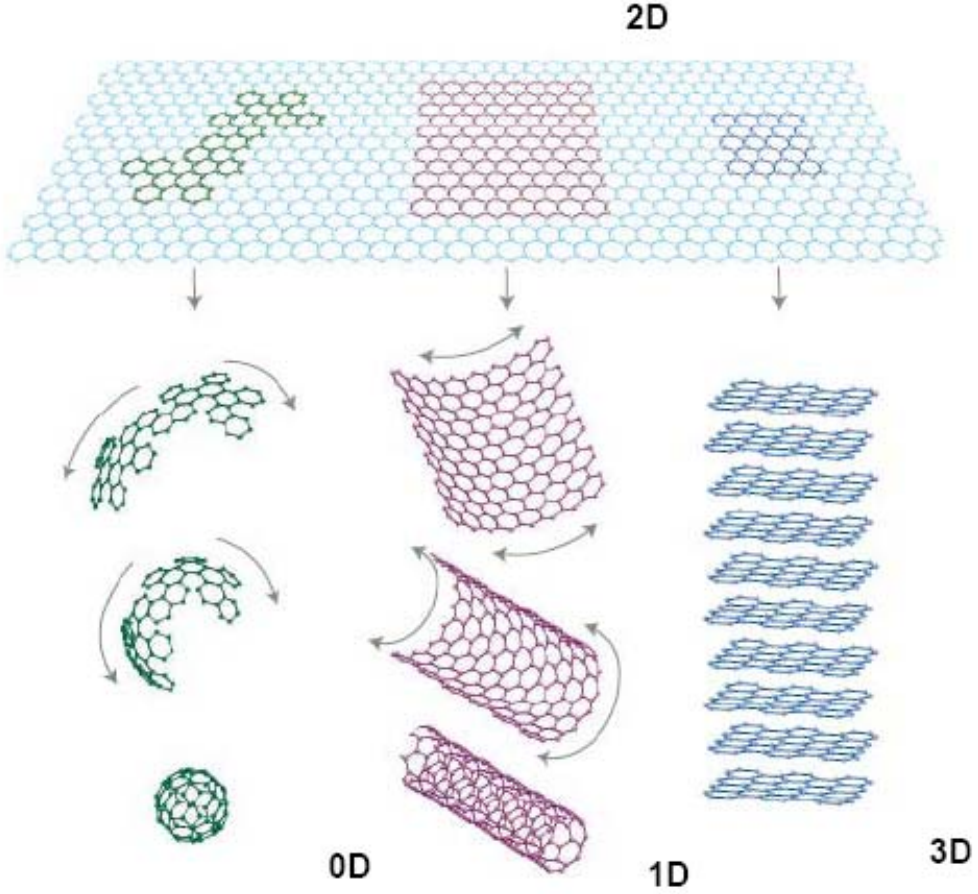

Graphene is a 2D building block material for other sp^2 bonded carbon materials. It can be wrapped up into 0D fullerenes, rolled into 1D nanotubes or stacked into 3D graphite

from A. Geim

Graphitic Materical

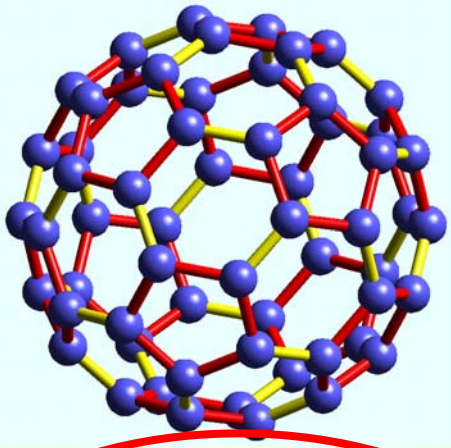

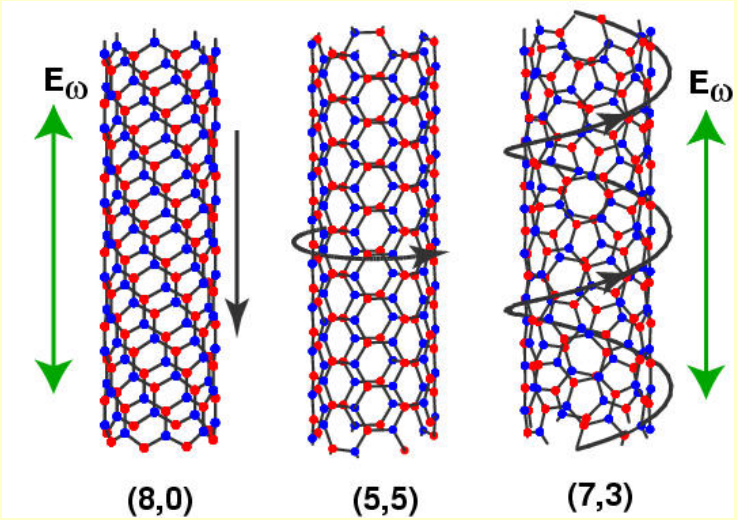

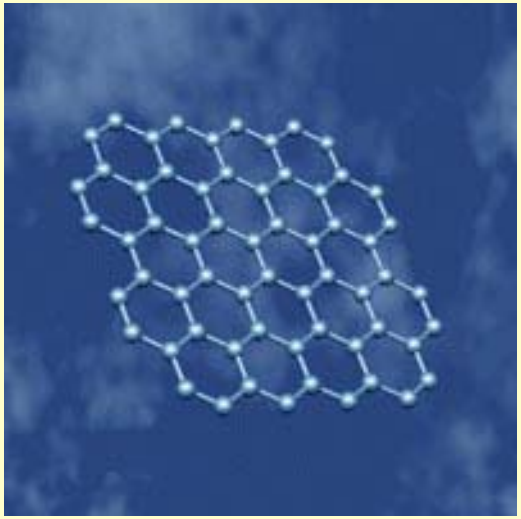

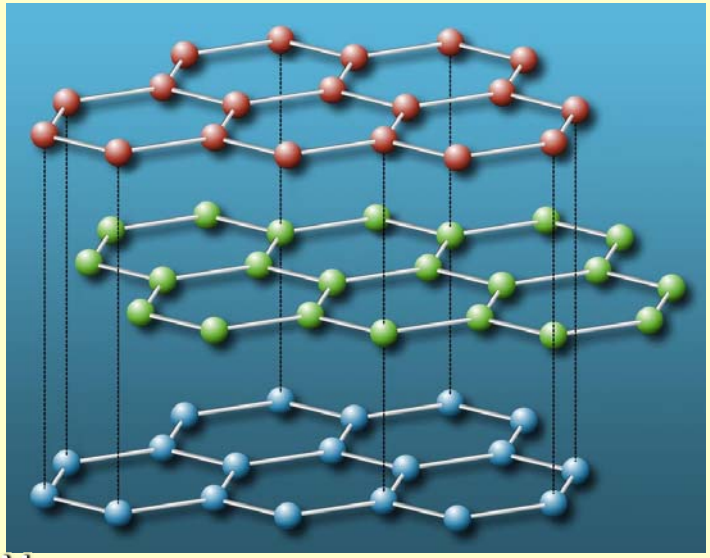

Graphitic devices

- Many graphene devices are similar to nanotube devices
- Current Graphene technology:
  - Mobility (~200000 cm^2/Vs) can be further improved
  - Ballistic transport on submicron scale
  - Gas sensors to detect small gas concentrations
- A band gap can be opened by quantum confinement effects on armchair graphene ribbons
- A band gap can be opened by placement of a graphene sample on a substrate, such as SiC to form a weak surface charge layer
- Spin polarization can be maintained over submicron distances
- Interesting proximity effects are observed in graphene when using superconducting and magnetic electrodes

Atomic Structure

Carbon has 4 electrons in the outer s-p shell

sp^2 hybridisation forms strong directed bonds which determine a honeycomb lattice structure.

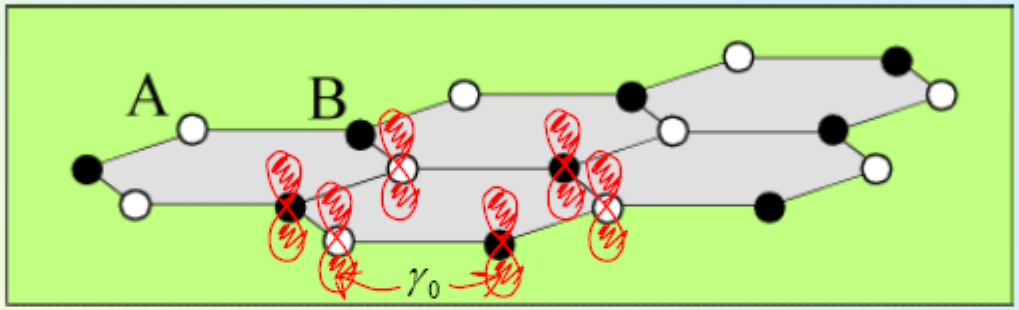

$p^z(\pi)$ orbitals determine conduction properties of graphite

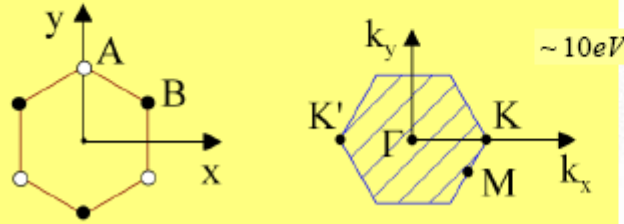

Two non-equivalent carbon positions

Two non-equivalent K-points

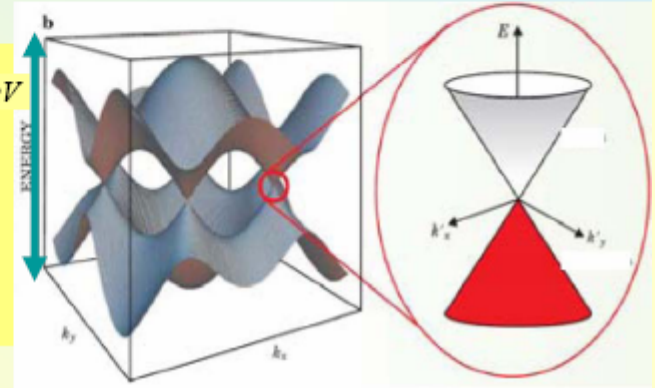

Reciprocal lattice in 3D:Review

• Semiconductors of interest to us have what is called a diamond structure. The diamond structure is composed of to interpenetrating FCC lattices the following way: Imagine two FCC lattices such that each atom of each lattice is on top of the corresponding atom of the other lattice. You should only be seeing 1 FCC lattice as of now. Then fix one lattice and move the other one in the direction of the body diagonal of the fixed one by ¼ of the body diagonal. Now you've yourself a diamond lattice. If the two FCC lattices are made up of two different types of atoms, the structure is then called a Zinchblend lattice.
• To visualize the reciprocal lattice **focus only on one FCC lattice** in the diamond structure.

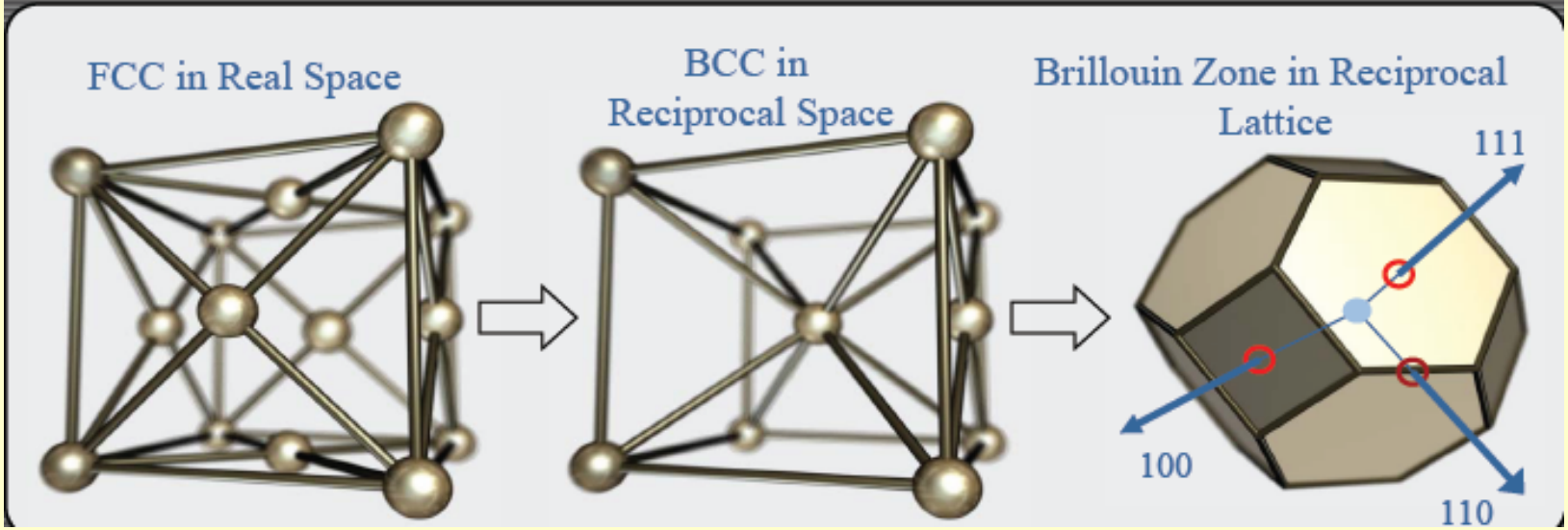

Dispersion Relation in 3D

• Since the reciprocal space is now 3 dimensional, to draw the E-k diagram we have choose particular directions and draw E-k diagram along those directions:

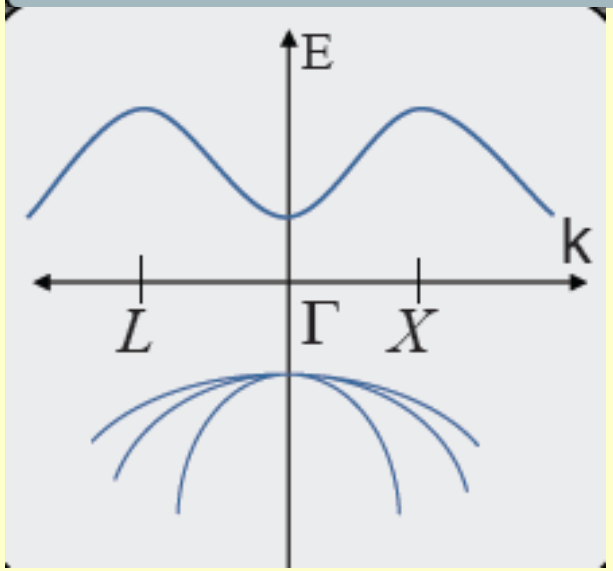

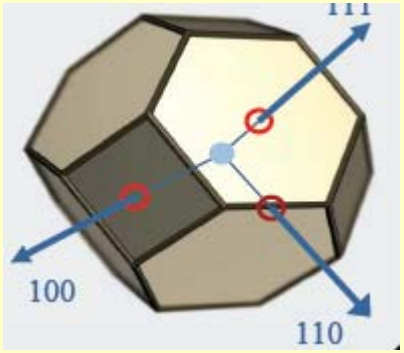

• Some useful information:
• The top of the valence band usually occurs at the Gamma point (k=0). The bottom of conduction band however does not always lie at k=0. For example consider Silicon:

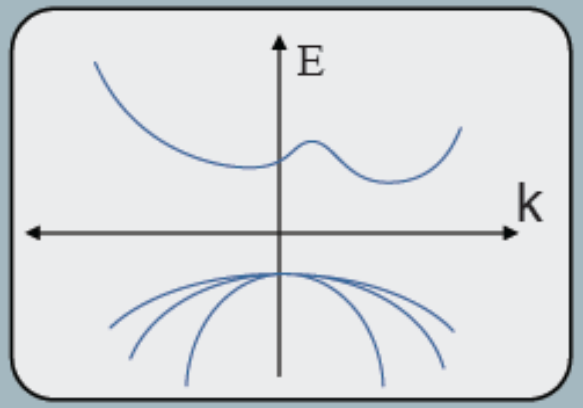

• If both conduction band minimum and the valence band maximum lie at the same value of k, the material is called a direction bandgap semiconductor. Other wise the material is indirect like Si.

Band Energy Effective Mass

- Usually, it is necessary to derive an expression for E(k_x, k_y, k_z) about the conduction points of a bulk solid

- For silicon, use the parabolic approximation

$$E = E_c + \frac{\hbar^2 k^2}{2m^*} = \frac{\hbar^2 (k_x^{\,2} + k_y^{\,2} + k_z^{\,2})}{2m^*}$$

where m* is the effective mass.

- For nanotubes we can derive a similar parabolic expression via a Taylor series expansion that approximates the subbands near the conduction valleys

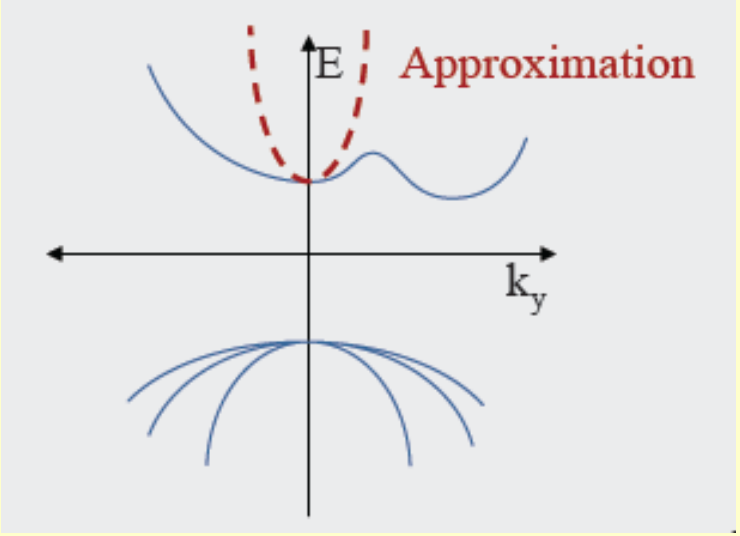

Dispersion Relation in Graphene

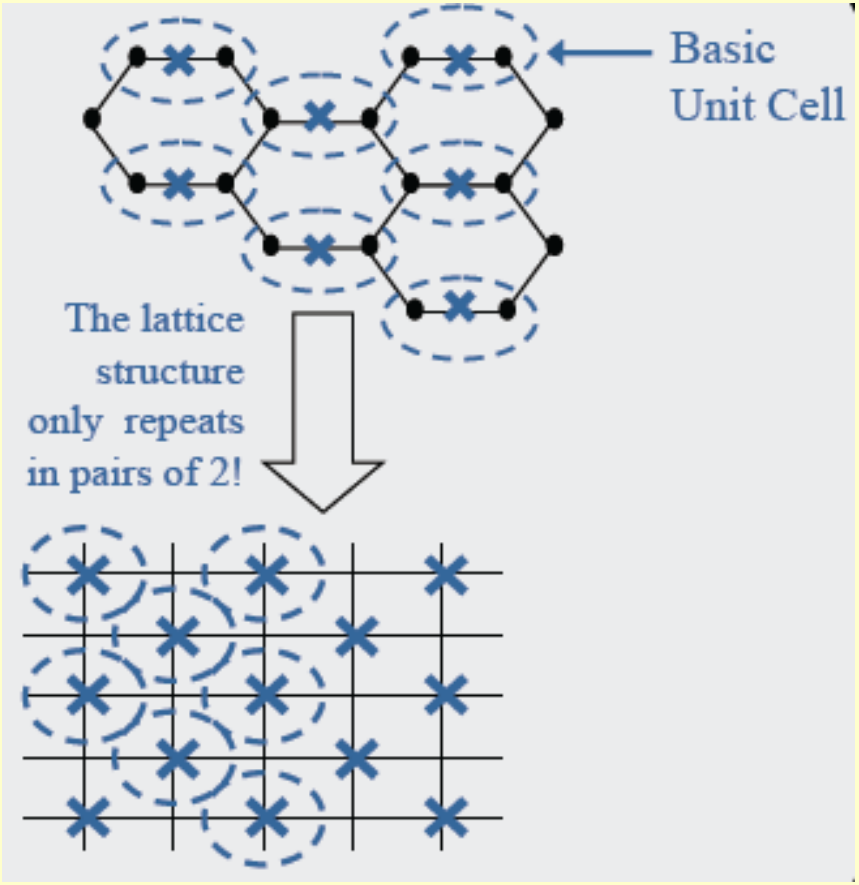

• Remember the general result of principle of bandstructure:

$$E\{\phi_0\} = \left[h(\vec{k})\right]\{\phi_0\}$$

$$\left[h(\vec{k})\right] = \sum_m \left[H_{nm}\right] e^{i\vec{k}\bullet(\vec{d}_m - \vec{d}_n)}$$

• To write h(k) consider one unit cell an its nearest neighbors. Figure shows that there will be 5 terms in the summation for h(k).

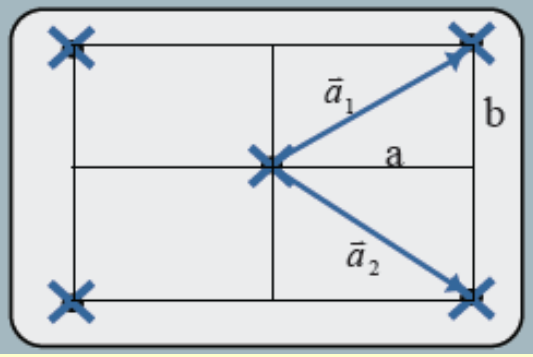

Dispersion Relation in Graphene

• Remember the general result of principle of bandstructure:

$$E\{\phi_0\} = \left[h\left(\vec{k}\right)\right]\{\phi_0\}$$

$$\left[h\left(\vec{k}\right)\right] = \sum_m \left[H_{nm}\right] e^{i\vec{k}\bullet\left(\vec{a}_m - \vec{a}_n\right)}$$

•To write h(k) consider one unit cell an its nearest neighbors. Figure shows that there will be 5 terms in the summation for h(k).

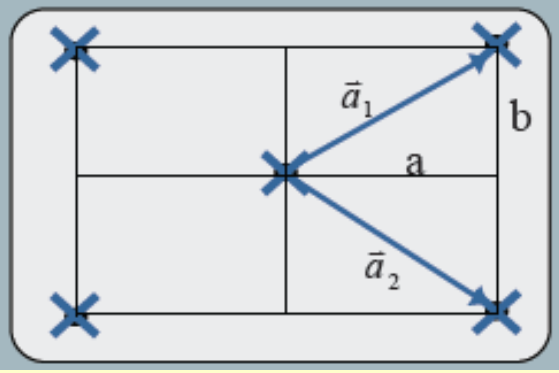

• Writing the summation terms and adding them up we get:

$$h(\vec{k}) = \begin{bmatrix} \varepsilon & h_0^* \\ h_0 & \varepsilon \end{bmatrix}$$

• Where

$$h_0 = t\left(1 + e^{i\vec{k}\cdot\vec{a}_1} + e^{i\vec{k}\cdot\vec{a}_2}\right)$$

• The eigenvalues of this matrix are given by:

$$E\left(\vec{k}\right) = \varepsilon \pm \left|h_0\left(\vec{k}\right)\right|$$

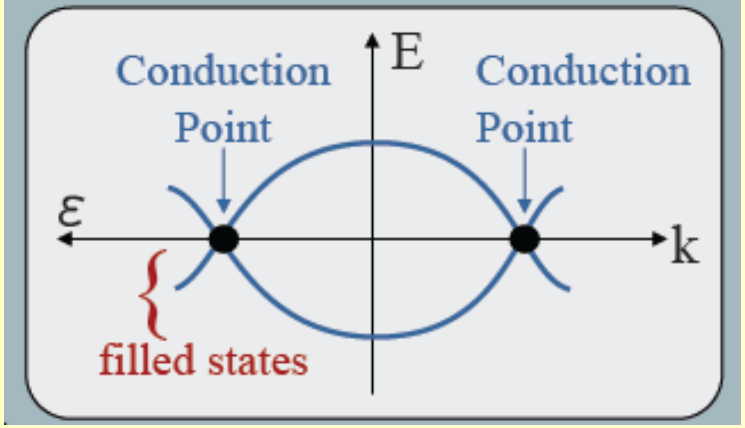

• Next we like to locate the conduction points in the 2 dimensional k space:

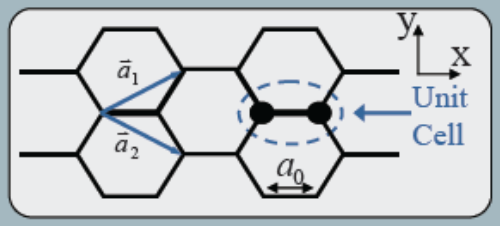

$$\vec{a}_1 = a\hat{x} + b\hat{y} = \tfrac{3}{2} a_0 \hat{x} + \tfrac{\sqrt{3}}{2} a_0 \hat{y}$$

$$\vec{a}_2 = a\hat{x} - b\hat{y} = \tfrac{3}{2} a_0 \hat{x} - \tfrac{\sqrt{3}}{2} a_0 \hat{y}$$

$$\vec{k} = k_x \hat{x} + k_y \hat{y}$$

$$h_0 = t\left(1 + e^{i\vec{k}\cdot\vec{a}_1} + e^{i\vec{k}\cdot\vec{a}_2}\right) = t\left(1 + e^{i(k_x a + k_y b)} + e^{i(k_x a - k_y b)}\right) = t\left(1 + 2e^{ik_x a}\cos k_y b\right)$$

• To find the conduction points we need to set |h(k)|=0. So we need to find |h(k)|:

$$\therefore |h_0|^2 = h_0 h_0^* = t^2\left(1 + 4\cos k_x a \cos k_y b + 4\cos^2 k_y b\right)$$

so,

$$|h_0(\vec{k})| = t\sqrt{1 + 4\cos k_x a \cos k_y b + 4\cos^2 k_y b}$$

• Now let $|h_0(\vec{k})| = t\sqrt{1 + 4\cos k_x a \cos k_y b + 4\cos^2 k_y b} = 0$

• Let kxa=0 and investigate h(k) as a function of ky.

$$h_0 = t\left(1 + 2\cos k_y b\right) \text{ for } k_x = 0 \Rightarrow k_y b = \frac{2\pi}{3} \text{ to get } h_0(k) = 0$$

• Let kxa=pi and investigate h(k) as a function of ky.

$$h_0 = t\left(1 - 2\cos k_y b\right) \text{ for } k_x = \pi \Rightarrow k_y b = \frac{\pi}{3} \text{ to get } h_0(k) = 0$$

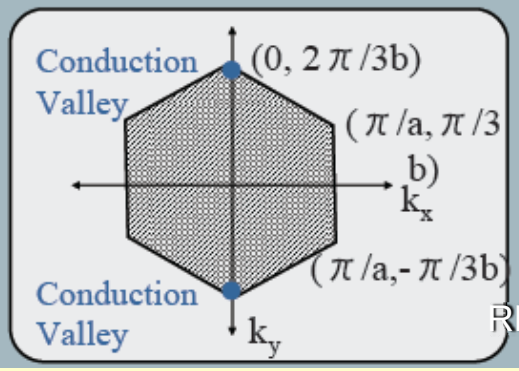

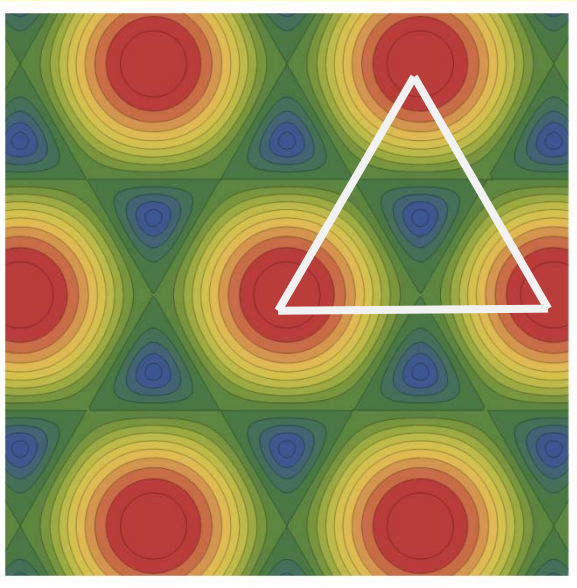

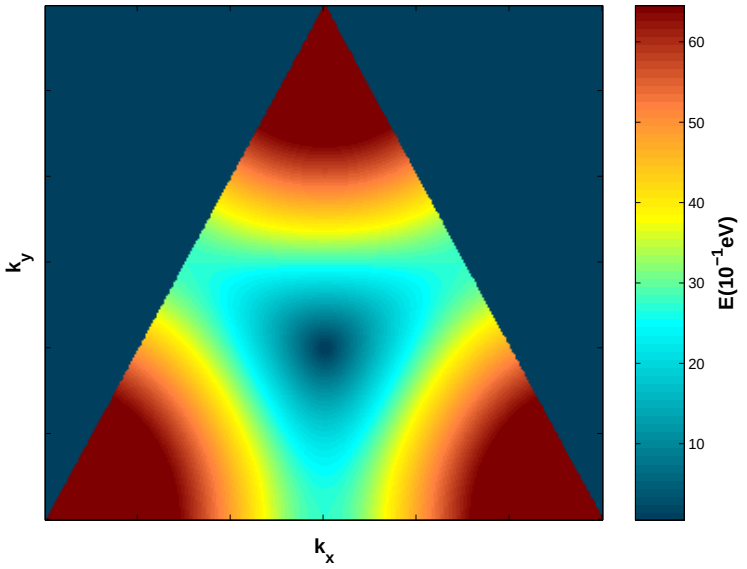

Valley Degeneracy

• The six Brillouin valleys really only give 2 independent valleys, e.g. in each group of 3 that are in the picture two of the valleys are away form the other by a reciprocal lattice unit vector; hence represent the same state. One can think that each corner in the 1st Brillouin zone contributes 1/3rd.1/3 x 6 = 2(left figure). Alternatively we can translate two of the corners in each group to get the full valleys on the right.

Dispersion relation along ky.

$$h_0 = t\left(1 + 2\cos k_y b\right) \text{ for } k_x = 0$$

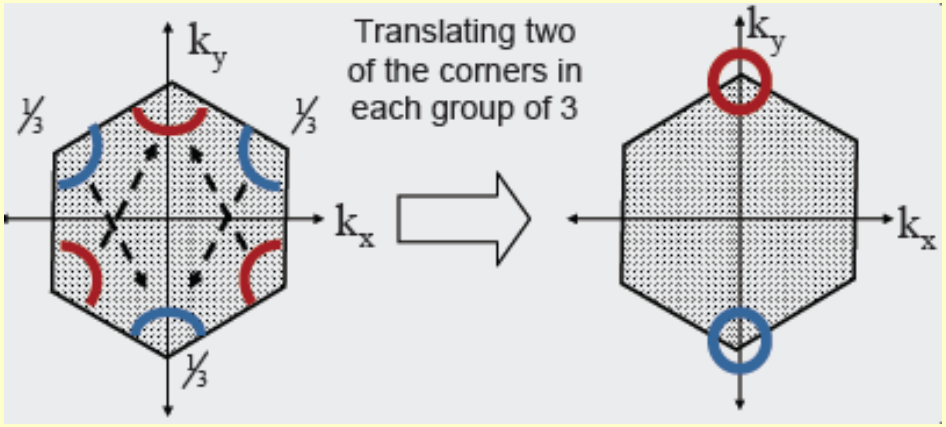

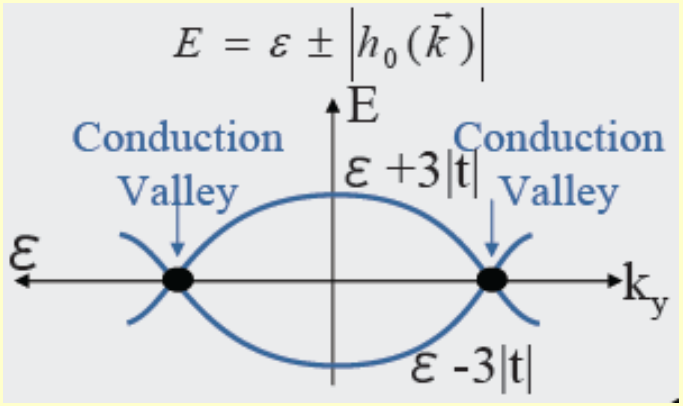

Review: C2DES vs 2DEG

Graphene

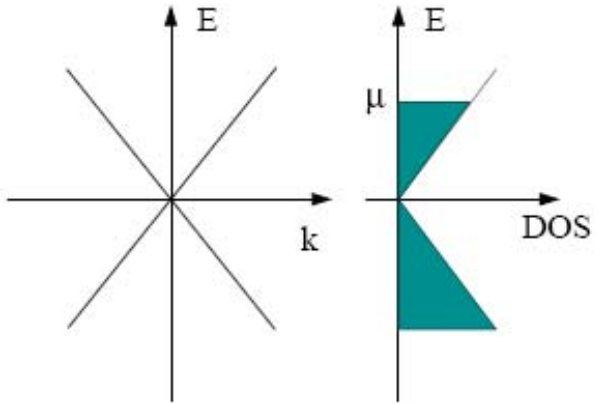

- $E(\mathbf{k}, \lambda) = \lambda \hbar \mathbf{v_F} \mathbf{k}$, no gap
- $DOS(E) := 1/A \partial N/\partial E \propto E$
- Two valleys *s* and spinor wavefunction (A,B)

2DEG

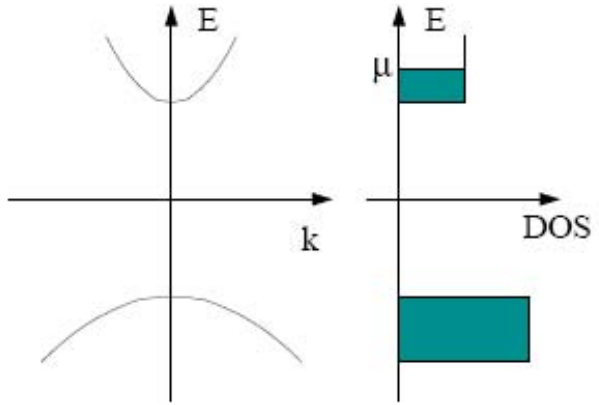

- $E(\mathbf{k}, \lambda) = \frac{\hbar^2 \mathbf{k}^2}{2\mathbf{m}^*}$, gap (1.4 eV for GaAs)
- $DOS(E) = const$
- Eigenfunctions are plane waves

Review: Mono- and Bi-layer

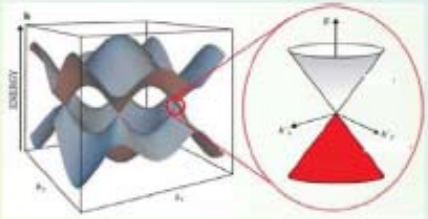

Wallace, Phys. Rev. 71, 622 (1947)

Monolayer and bilayer graphene

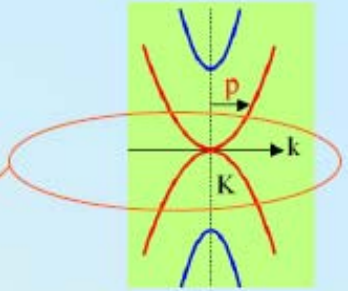

McCann, VF - PRL 96, 086805 (2006)

$$\hat{H}_1 \approx v\vec{p}\cdot\vec{\sigma}$$

$$\hat{H}_2 \approx \frac{(p_y^2 - p_x^2)\sigma_x - 2p_x p_y \sigma_y}{2m}$$

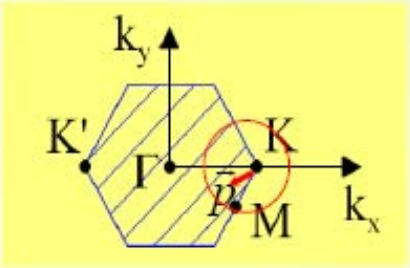

$$\psi = \begin{pmatrix} \psi_A \\ \psi_B \end{pmatrix}$$

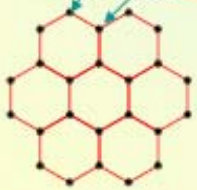

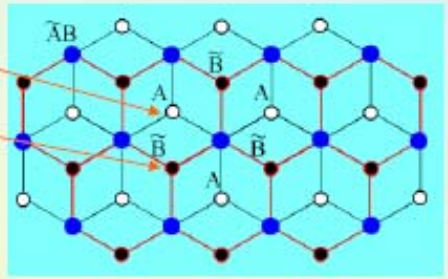

Bloch function amplitudes on the AB sites - 'isospin'

Pseudospin

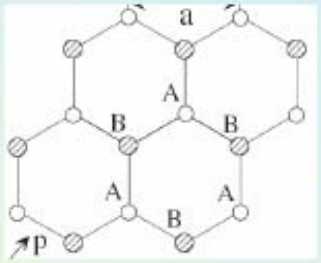

valley index
'pseudospin'

$$\hat{H} = \begin{pmatrix} 0 & \pi^+ & & \\ \pi & 0 & & \\ & & 0 & -\pi^+ \\ & & -\pi & 0 \end{pmatrix} \begin{pmatrix} \varphi_{A,+} \\ \varphi_{B+} \\ \varphi_{B-} \\ \varphi_{A-} \end{pmatrix}$$

$$\pi = p_x + ip_y$$

$$\pi^+ = p_x - ip_y$$

sublattice index
'isospin'

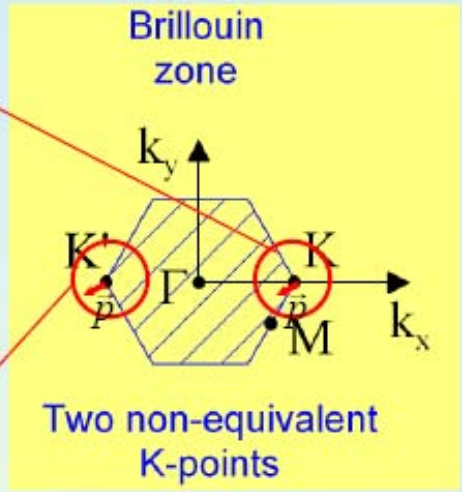

Also, one may need to take into account an additional real spin degeneracy of all states

Chirality

Bloch function amplitudes (e.g., in the valley K) on the AB sites ('isospin') mimic spin components of a relativistic particle.

$$\hat{H} = v\begin{pmatrix} 0 & p_x - ip_y \\ p_x + ip_y & 0 \end{pmatrix} = v\vec{\sigma}\cdot\vec{p} \qquad \psi = \begin{pmatrix} \psi_A \\ \psi_B \end{pmatrix}$$

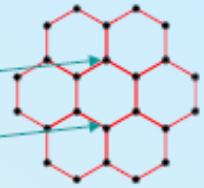

Chiral Dirac-type (relativistic) electrons: isospin of plane waves is linked to the momentum direction, which determines unusual transport properties of graphene.

$$\varepsilon = vp$$

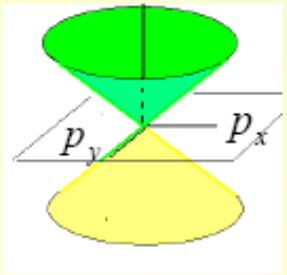

conduction band

$\vec{\sigma}\cdot\vec{n} = 1$ → $\vec{p}$

$\vec{\sigma}\cdot\vec{n} = -1$ ← $\vec{p}$

valence band

$$\vec{p} = (p\cos\varphi, p\sin\varphi)$$

$$\psi_{\vec{p}} = \frac{1}{\sqrt{2}}\begin{pmatrix} e^{i\varphi/2} \\ \pm e^{-i\varphi/2} \end{pmatrix}$$

chiral plane wave states

How do we determine Fermi Surface?

Electron 'chirality' and ARPES in graphene

$$H_1 = v\vec{p}\cdot\vec{\sigma} = vp\begin{pmatrix} 0 & e^{-i\varphi} \\ e^{i\varphi} & 0 \end{pmatrix} \Rightarrow \pm vp$$

$$\psi_{\pm} = \begin{pmatrix} \psi_A \\ \psi_B \end{pmatrix} = \frac{1}{\sqrt{2}}\begin{pmatrix} e^{-i\varphi/2} \\ \pm e^{i\varphi/2} \end{pmatrix}$$

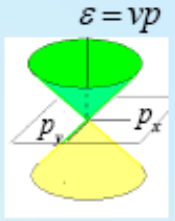

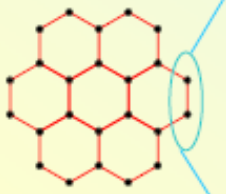

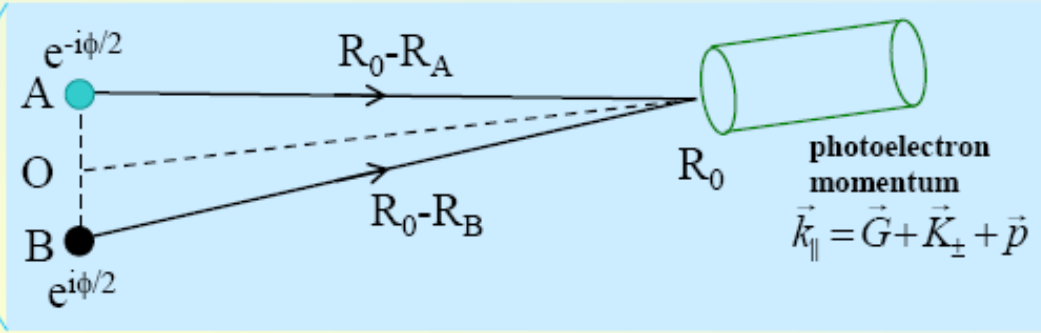

$$I_{\pm} \sim \left| e^{i\vec{k}\cdot(\vec{R}_0 - \vec{R}_A) - i\varphi/2} \pm e^{i\vec{k}\cdot(\vec{R}_0 - \vec{R}_B) + i\varphi/2} \right|^2 = \left| e^{\frac{i}{2}\vec{k}\cdot(\vec{R}_A - \vec{R}_B + \varphi)} \pm e^{-\frac{i}{2}\vec{k}\cdot(\vec{R}_A - \vec{R}_B + \varphi)} \right|^2$$

Evidence: Exp. Observation

Electron 'chirality' and ARPES in graphene

Relative phase on sub-lattices due to the electron chirality in graphene makes each pattern anisotropic. Thus, ARPES give a direct image of chiral states.

$$\varepsilon = -vp$$

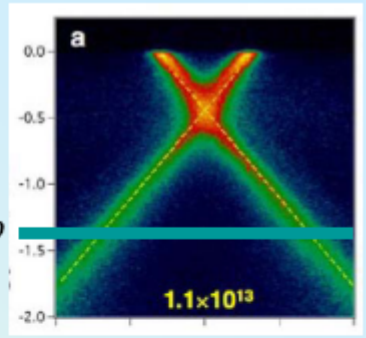

$$\vec{k}_{\parallel} = \vec{G} + \vec{K}_{\pm} + \vec{p}$$

$$I \sim \sin^2\left(\frac{\vec{k}\cdot\left(\vec{R}_A - \vec{R}_B\right)}{2} + \frac{\varphi}{2}\right)$$

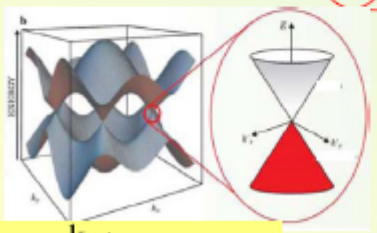

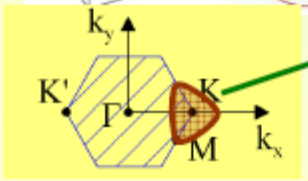

trigonal warping

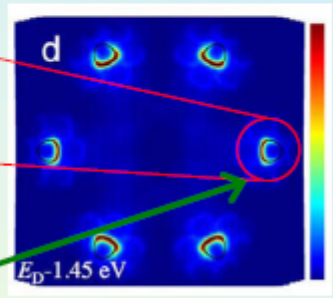

Bostwick, Ohta, Seyller, Horn, Rotenberg
Nature Physics 3, 36 (2007)

Bilayer Graphene

Electrons in bilayer graphene

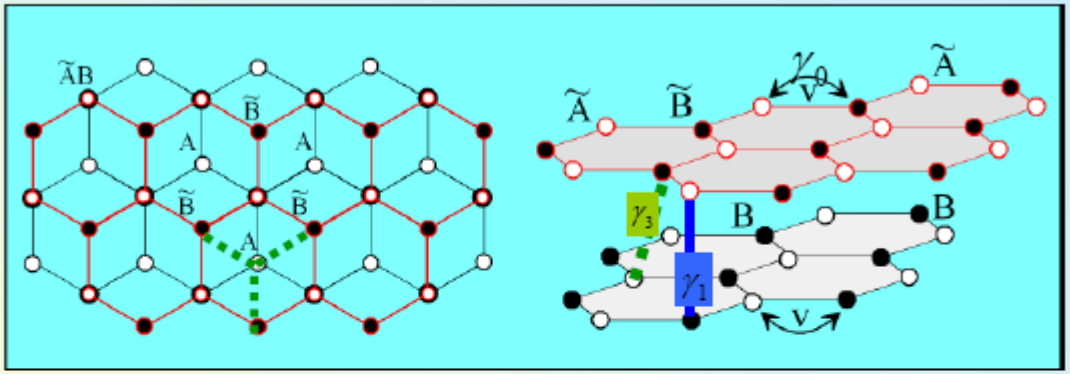

Slonczewski-Weiss-McClure parameterization for Bernal stacking

$$H_2 = \begin{pmatrix} 0 & v_3\pi & 0 & v\pi \\ v_3\pi^+ & 0 & v\pi^+ & 0 \\ 0 & v\pi & 0 & \gamma_1 \\ v\pi^+ & 0 & \gamma_1 & 0 \end{pmatrix}$$

$$v_3 = -\frac{\sqrt{3}}{2}\frac{\gamma_3 a}{\hbar}$$

Summary

Summary of band structure: chiral electrons in monolayer and bilayer graphene

$$H_1 = \varsigma v \begin{pmatrix} 0 & \pi^+ \\ \pi & 0 \end{pmatrix} + \mu \begin{pmatrix} 0 & \pi^2 \\ (\pi^+)^2 & 0 \end{pmatrix}$$

$$\begin{pmatrix} A \\ B \\ B \\ A \end{pmatrix} \begin{matrix} \varsigma=+1 \\ \varsigma=-1 \end{matrix}$$

valley

'trigonal warping' terms

$$H_2 = \frac{1}{2m} \begin{pmatrix} 0 & (\pi^+)^2 \\ \pi^2 & 0 \end{pmatrix} + \varsigma v_3 \begin{pmatrix} 0 & \pi \\ \pi^+ & 0 \end{pmatrix}$$

$$\begin{pmatrix} A \\ \tilde{B} \\ \tilde{B} \\ A \end{pmatrix} \begin{matrix} \varsigma=+1 \\ \varsigma=-1 \end{matrix}$$

dominant at intermediate energies

$$\pi = p_x + ip_y = pe^{i\varphi} \qquad \pi^+ = p_x - ip_y = e^{i\varphi}$$

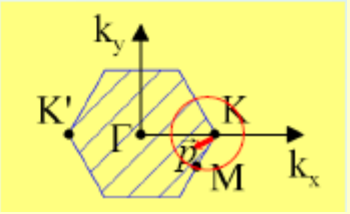

Summary

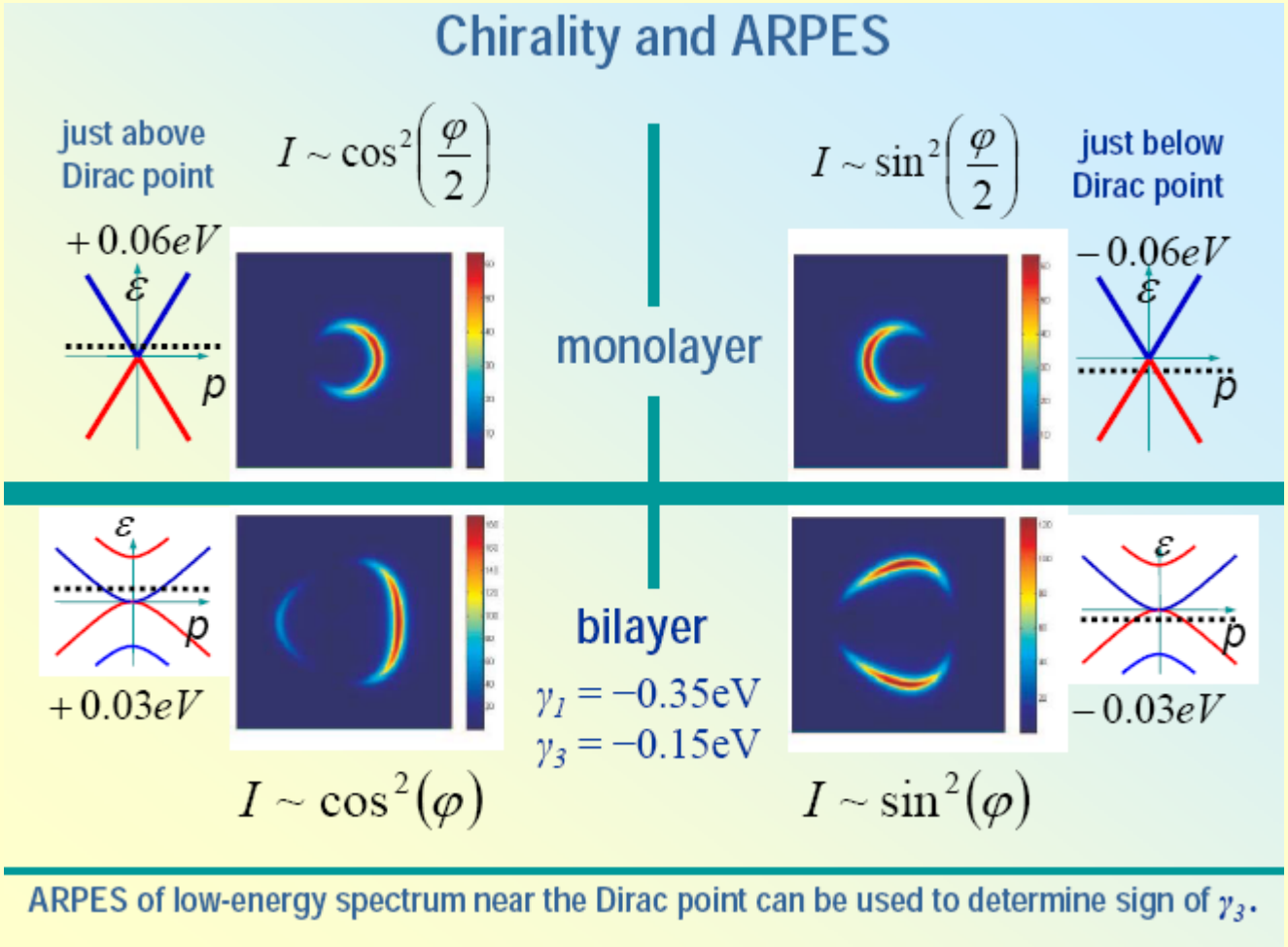
Chirality and ARPES
just above Dirac point
$I \sim \cos^2\left(\frac{\varphi}{2}\right)$
$I \sim \sin^2\left(\frac{\varphi}{2}\right)$
just below Dirac point
$+0.06eV$
$-0.06eV$
ε
p
monolayer
bilayer
$\gamma_1 = -0.35\text{eV}$
$\gamma_3 = -0.15\text{eV}$
$+0.03eV$
$-0.03eV$
$I \sim \cos^2(\varphi)$
$I \sim \sin^2(\varphi)$
ARPES of low-energy spectrum near the Dirac point can be used to determine sign of γ_3.

Gapped Graphene

$$\Delta = \varepsilon_A - \varepsilon_B$$

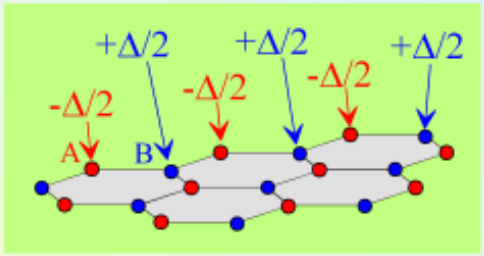

Substrate-induced AB asymmetry

$$H = \begin{pmatrix} -\Delta/2 & vpe^{-i\varphi} \\ vpe^{i\varphi} & \Delta/2 \end{pmatrix}$$

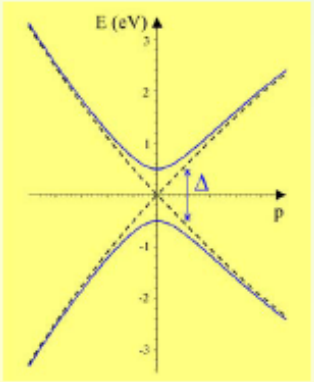

Energy fixed at $-0.2eV$

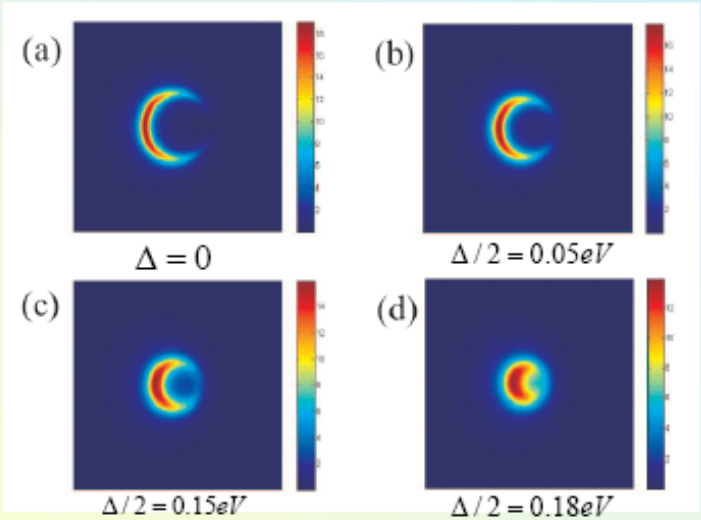

Transport in Graphene

Interference correction: weak localisation effect…

$$w \sim |A_{\subset} + A_{\supset}|^2 = |A_{\subset}|^2 + |A_{\supset}|^2 + [A_{\subset}^* A_{\supset} + A_{\subset} A_{\supset}^*]$$

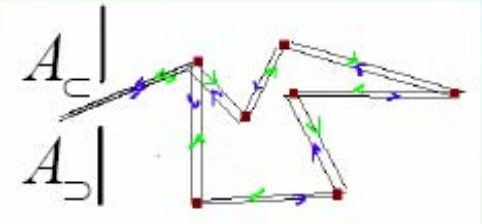

$$e^{i\varphi_{\supset}} = e^{i\varphi_{\subset}} \qquad A_{\supset} = A_{\subset}$$

$$A_{\subset}^* A_{\supset} = |A_{\subset}|^2 > 0$$

$$\sigma = \sigma_{cl} - \frac{e^2}{2\pi h} \ln(\tau_{\varphi} / \tau)$$

WL = enhanced backscattering in time-reversal-symmetric systems

Transport in Graphene

... but ...

$$w \sim |A_{\circlearrowleft} + A_{\circlearrowright}|^2 = |A_{\circlearrowleft}|^2 + |A_{\circlearrowright}|^2 + [A_{\circlearrowleft}^* A_{\circlearrowright} + A_{\circlearrowleft} A_{\circlearrowright}^*]$$

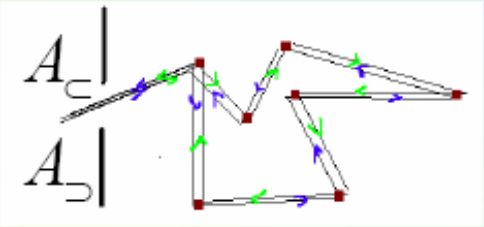

WL = enhanced backscattering for non-chiral electrons in time-reversal-symmetric systems

WAL = suppressed backscattering for Berry phase π electrons

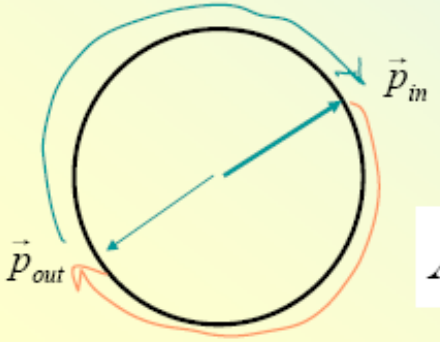

chiral electrons $\psi_{out} = e^{-i\phi(\sigma_z/2)}\psi_{in}$

$$A_{\circlearrowleft} A_{\circlearrowright}^* = e^{-i2\pi(\sigma_z/2)} |A_{\circlearrowleft}|^2 = -|A_{\circlearrowleft}|^2 < 0$$

Transport in Graphene

... but ...

$$w \sim |A_{\circlearrowleft} + A_{\circlearrowright}|^2 = |A_{\circlearrowleft}|^2 + |A_{\circlearrowright}|^2 + [A^*_{\circlearrowleft} A_{\circlearrowright} + A_{\circlearrowleft} A^*_{\circlearrowright}]$$

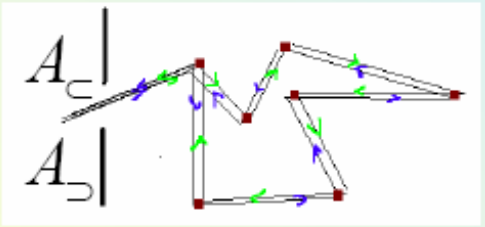

WL = enhanced backscattering for non-chiral electrons in time-reversal-symmetric systems

$$\sigma = \sigma_{ci} + \frac{e^2}{2\pi h} \ln\left(\min[\tau_\varphi, \tau_B]/\tau\right)$$

WAL = suppressed backscattering for Berry phase π electrons

chiral electrons $\psi_{out} = e^{-i\phi(\sigma_z/2)} \psi_{in}$

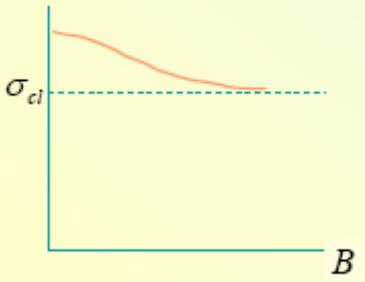

$$A_{\circlearrowleft} A^*_{\circlearrowright} = e^{-i2\pi(\sigma_z/2)} |A_{\circlearrowleft}|^2 = -|A_{\circlearrowleft}|^2 < 0$$

Suzuura, Ando - PRL 89, 266603 (2002)

Transport in Graphene

... however ...

weak trigonal warping leads to a random phase difference, δ for long paths.

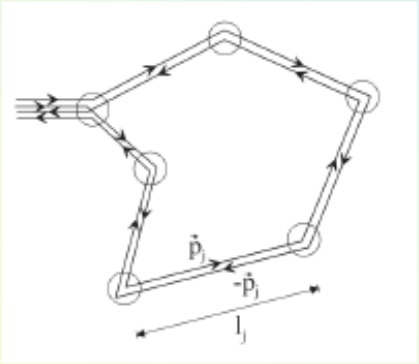

$$\hat{H} = \varsigma v \vec{\sigma} \cdot \vec{p} - \mu\left((p_x^2 - p_y^2)\sigma_x - 2p_x p_y \sigma_y\right) + \hat{I}u(\vec{r})$$

$$e^{i\delta} A_{\circlearrowright}^{(0)} \neq e^{-i\delta} A_{\circlearrowleft}^{(0)}$$

$$\delta = \sum_j \left[\varepsilon(\vec{p}_j) - \varepsilon(-\vec{p}_j)\right] l_j / \hbar v_F$$

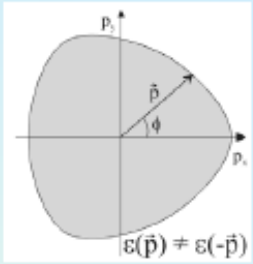

$$\sigma = \sigma_{ci} + \frac{e^2}{2\pi h} \ln\left(\min[\tau_\varphi, \tau_B]/\tau\right)$$

Some types of disorder lead to a similar effect.

chiral electrons $\psi_{out} = e^{-i\phi(\sigma_z/2)} \psi_{in}$

$$A_{\circlearrowleft} A_{\circlearrowright}^* = e^{-i2\pi(\sigma_z/2)} |A_{\circlearrowleft}|^2 = -|A_{\circlearrowleft}|^2 < 0$$

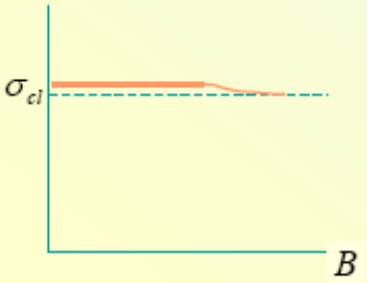

McCann, Kechedzhi, VF, Suzuura, Ando, Altshuler - PRL 97, 146805 (2006)
for bilayers: Kechedzhi, McCann, VF, Altshuler – PRL 98, 176806 (2007)

Dirac Massless: Evidence

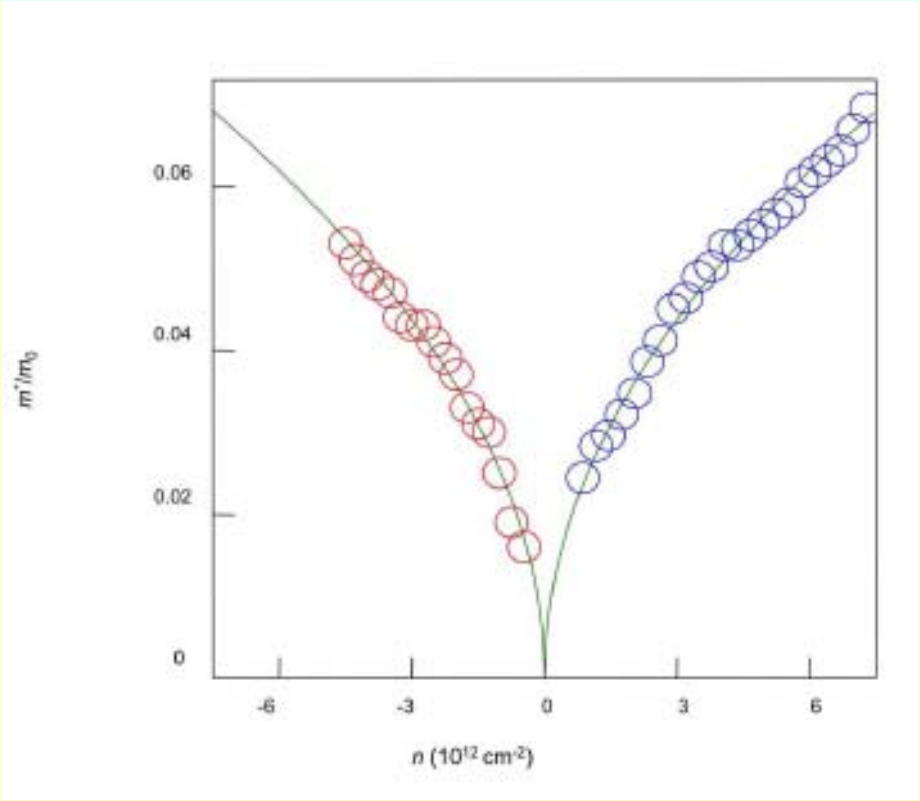

$$m^* = \frac{1}{2\pi}\left[\frac{\partial A(E)}{\partial E}\right]_{E=E_F}$$

$$A(E) = \pi q(E)^2$$

$$m^* \approx \sqrt{n}$$

$$q = \sqrt{\pi\, n} \qquad \Rightarrow E = \pm\alpha\, q$$

Novoselov *et al* Nature 438,197 (2005)

Quantum transport measurements

Nature 438 (2005) 04233 Manchester group
Nature 438 (2005) 04235 Columbia group

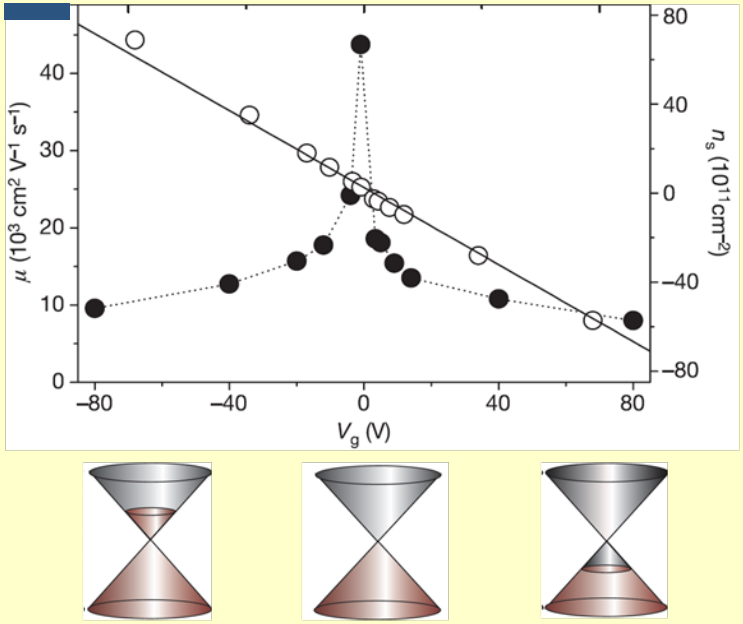

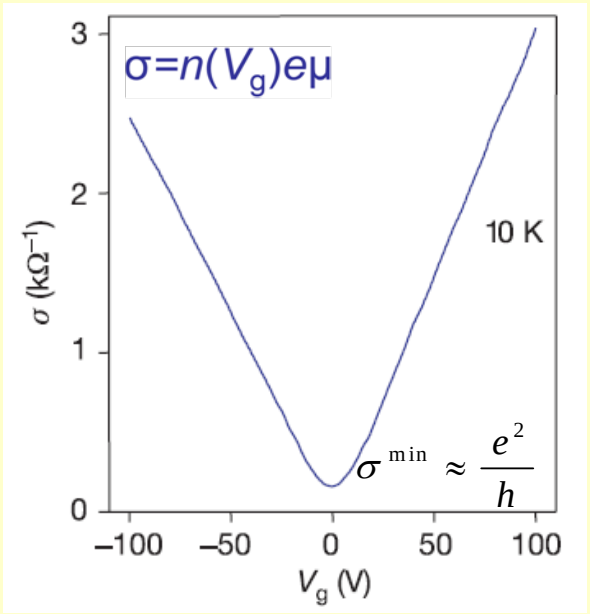

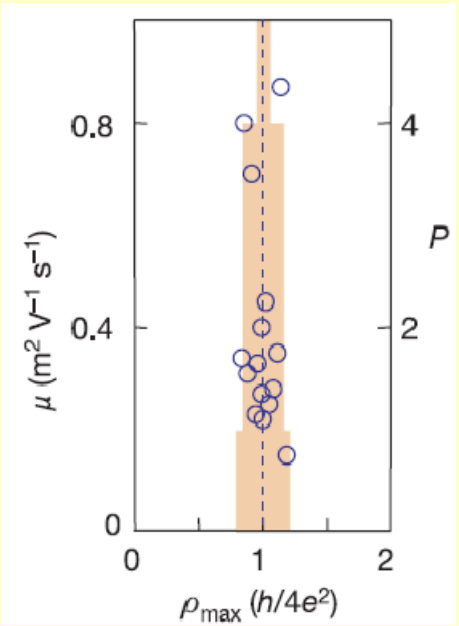

$\sigma_0^s = (e^2/h)\ (2E_F\tau_0/\hbar) =$ $\sigma_0^s = Const$ $V(\mathrm{r}) = \sum_I^{N_i} e^2/\epsilon|\mathrm{r}-\mathbf{R}_I|$

$\sigma_0^c \simeq (4e^2/h)\ (n/n_i)\ 32/\pi$

$\hbar/\tau_0 = 2\pi V^2 \rho_F = (n_i u^2/\hbar v^2)\ |E_F|$ $(2\pi e^2)/\epsilon(q + 4\alpha_g k_F) \simeq (\hbar v \pi)/(2k_F)$

$V(\mathrm{r}) = u\sum_I^{N_i} \delta(\mathrm{r}-\mathbf{R}_I)$

Quantum transport

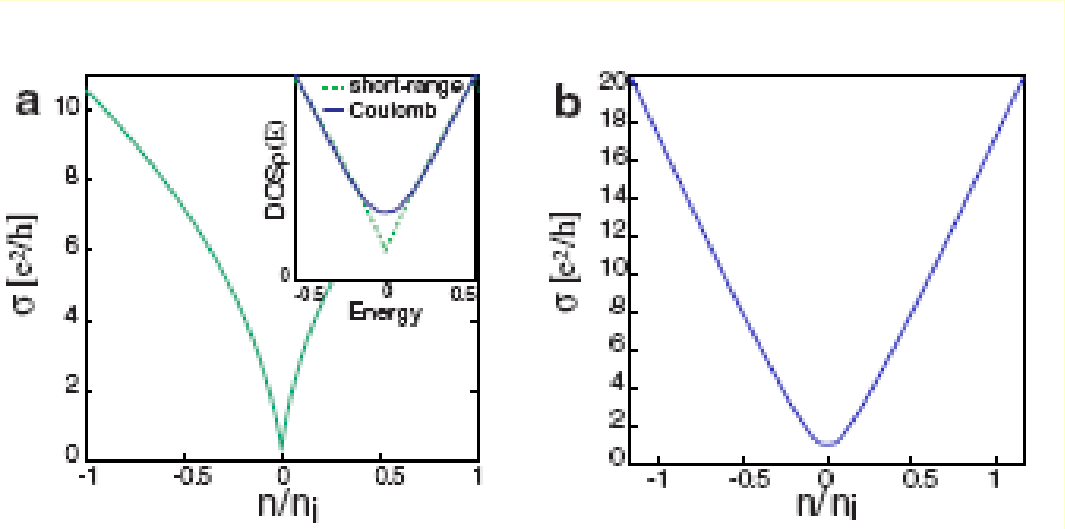

$$\sigma = -\frac{i\hbar e^2}{L^2}\sum_{n,n'}\frac{f(E_n)-f(E_{n'})}{E_n-E_{n'}}\frac{\langle n|v_x|n'\rangle\langle n'|v_x|n\rangle}{E_n-E_{n'}+i\eta},$$

$$[-i\hbar v\boldsymbol{\sigma}\cdot\nabla+V(\mathbf{r})]\psi = E\psi,$$

K. Namura and A. H. MacDonald PRL **98**,076602 (2007)

Minimum Conductivity?

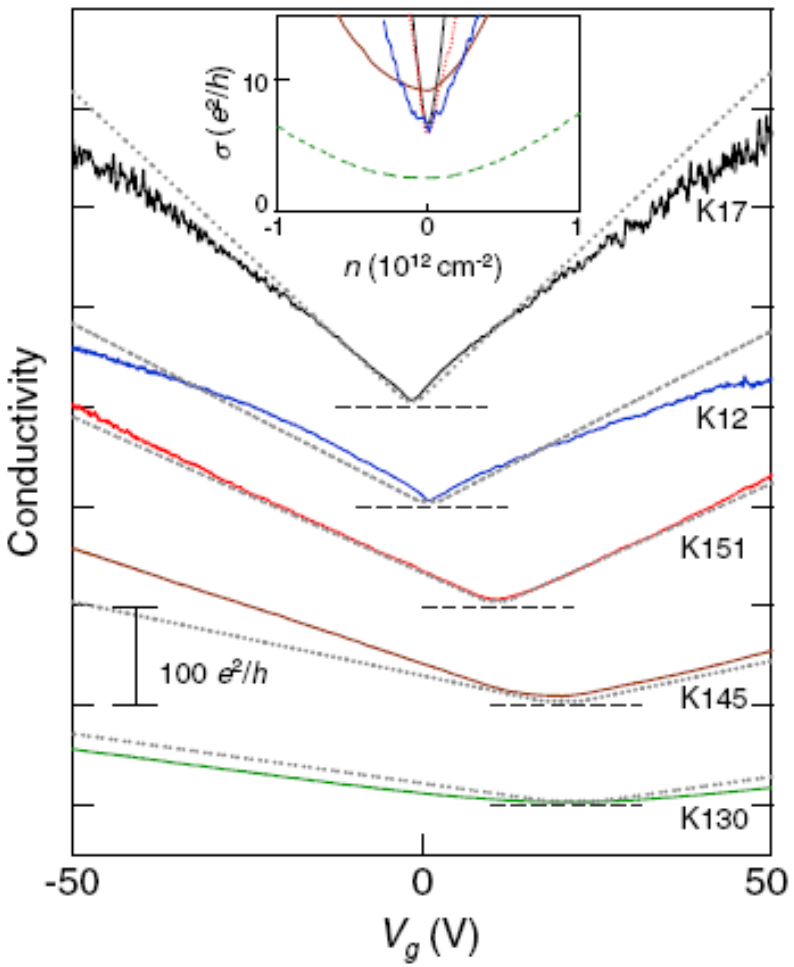

$$\sigma(V_g) \approx \begin{cases} C\frac{e^2}{h}\frac{n}{n_i} & \text{for } n > n^* \\ C\frac{e^2}{h}\frac{n^*}{n_i} & \text{for } n < n^*, \end{cases}$$

Tan *et al.* PRL **99**,246803 (2007)
Adam *et al* PNAS **104**, 18392 (2007)

Suspended graphene

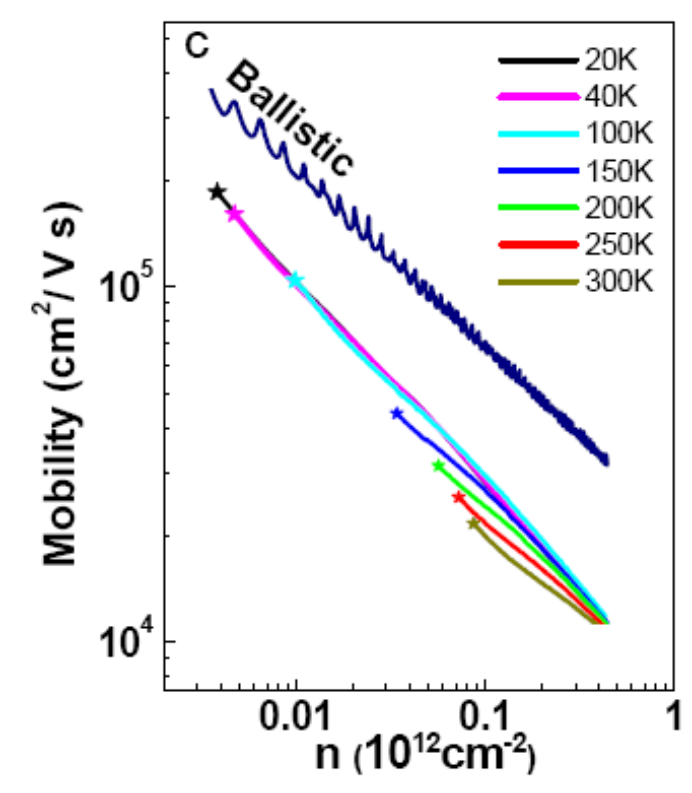

Xu Du *et al.* To appear in Nature (2008)

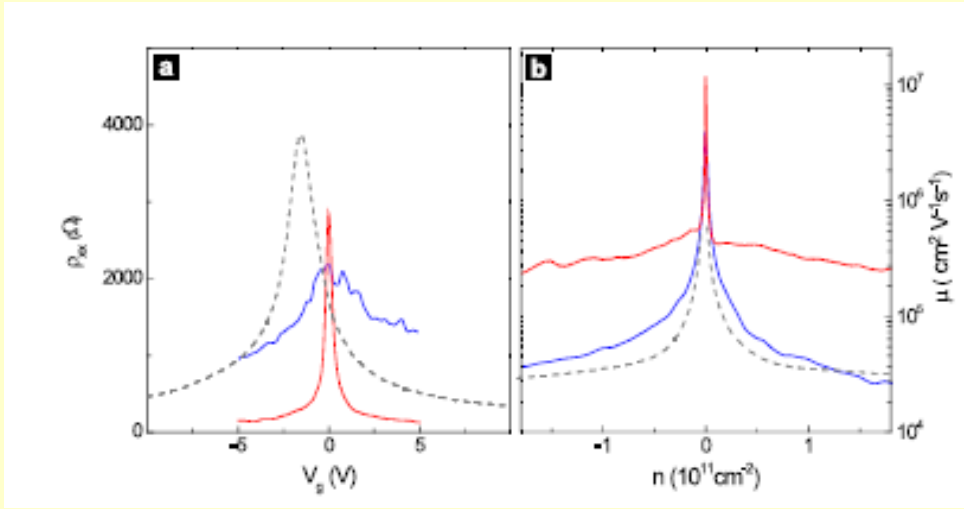

Bolotin *et al.* CM/0802.2389

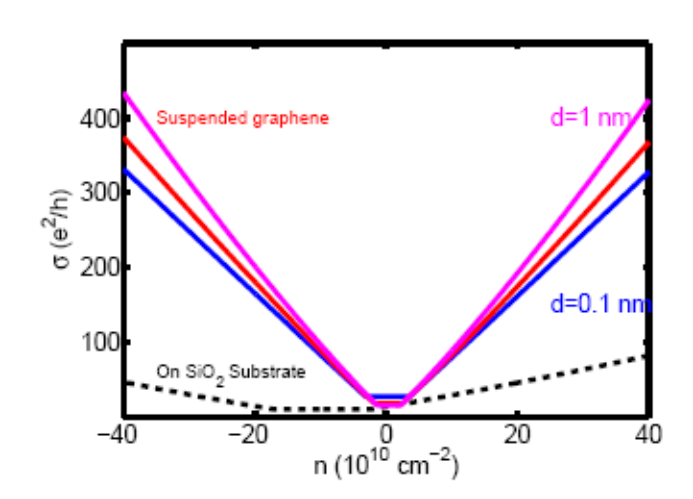

Adam and Das Sarma CM/0803.0735

Scattering mechanisms

- Charged impurities
- Neutral defects (short range scattering)
- Interface roughness
- Ripples
- Phonons, etc.

$$\mu_{charged} \approx \left(m_e^*\right)^{-1/2} T^{3/2}$$

$$\mu_{accousric\,mode} \approx \left(m_e^*\right)^{-5/2} T^{-3/2}$$

$$\mu_{optical\,mode} \approx \left(m_e^*\right)^{-5/2} T^{-1} \left[e^{\frac{\omega_{op}}{T}} - 1 \right]$$

$$\mu(T) \approx \begin{bmatrix} T \prec\prec 1 & 10^4 & (1978) \\ T \prec\prec 1 & 3\times 10^6 & (2000) \\ T = 300 & 2000 & (2000) \end{bmatrix}$$

2D Semiconductor

Chiral Linhard Function

$$\chi_{00}^{(0)}(\mathbf{q},\Omega,\mu\neq 0) \;=\; -i\int\frac{d^2\mathbf{k}}{(2\pi)^2}\int\frac{d\omega}{2\pi}\mathrm{Tr}[i\gamma_0 G^{(0)}(\mathbf{k}+\mathbf{q},\omega+\Omega,\mu\neq 0)i\gamma_0 G^{(0)}(\mathbf{k},\omega,\mu\neq 0)]$$

$$G^{(0)}(\mathbf{k},\omega,\mu\neq 0) \;=\; i\frac{-\omega\gamma_0+v\mathbf{k}\cdot\boldsymbol{\gamma}}{-\omega^2+v^2\mathbf{k}^2-i\epsilon}-\pi\frac{-\omega\gamma_0+v\mathbf{k}\cdot\boldsymbol{\gamma}}{v|\mathbf{k}|}\delta(\omega-v|\mathbf{k}|)\Theta(\mu-v|\mathbf{k}|)$$

$$\chi_{00}^{(0)}(\mathbf{q},\Omega,\mu=0)=\frac{q^2}{16\sqrt{v^2|\mathbf{q}|^2-\Omega^2}}\Theta(v^2|\mathbf{q}|^2-\Omega^2)+i\frac{q^2}{16\sqrt{\Omega^2-v^2|\mathbf{q}|^2}}\Theta(\Omega^2-v^2|\mathbf{q}|^2)$$

$$\begin{aligned}\chi_{00}^{(0)}(\mathbf{q},i\Omega,\mu\neq 0) \;&=\; \chi_{00}^{(0)}(\mathbf{q},i\Omega,\mu=0)+2\times\Re e\;\delta\chi_{00}^{(0)}(\mathbf{q},i\Omega)\Big|_{\mathrm{1st}}=\frac{\mu}{2\pi v^2}+\frac{q^2}{16\sqrt{\Omega^2+v^2q^2}}\\ &-\;\frac{q^2}{8\pi\sqrt{\Omega^2+v^2q^2}}\Re e\left[\arcsin\left(\frac{2\mu+i\Omega}{vq}\right)+\left(\frac{2\mu+i\Omega}{vq}\right)\sqrt{1-\left(\frac{2\mu+i\Omega}{vq}\right)^2}\right]. \qquad (29)\end{aligned}$$

$$\lim_{\Omega\to+\infty}\chi_{00}^{(0)}(\mathbf{q},i\Omega,\mu\neq 0)=\frac{q^2}{16\Omega}+\mathcal{O}\left(\frac{1}{\Omega^2}\right)$$

$$\lim_{q\to+\infty}\chi_{00}^{(0)}(\mathbf{q},0,\mu\neq 0)=\frac{q}{16v}$$

Chiral Linhard Function

$$\chi^0(\mathbf{q}, i\omega_n) = \frac{g_s g_v}{(2\pi)^2} \int d^2k \sum_{\lambda,\lambda'=\pm} f^{\lambda\,\lambda'}(\boldsymbol{k},\mathbf{q}) \frac{n_F(E^\lambda(\boldsymbol{k})) - n_F(E^{\lambda'}(\boldsymbol{k}+\boldsymbol{q}))}{E^\lambda(\boldsymbol{k}) - E^{\lambda'}(\boldsymbol{k}+\boldsymbol{q}) + i\hbar\omega_n}$$

$$f^{\lambda\,\lambda'}(\boldsymbol{k},\mathbf{q}) = \frac{1}{2}\left(1 + \lambda\,\lambda' \frac{k + q\cos\varphi}{|\boldsymbol{k}+\mathbf{q}|}\right)$$

- Summation over bonding and anti-bonding bands λ, λ', $E^\lambda(\boldsymbol{k}) = \lambda\hbar v_F k$
- Wavefunction overlaps $f^{\lambda\,\lambda'}(\boldsymbol{k},\mathbf{q})$
- Linear energy dispersion $E^\lambda(\boldsymbol{k}) = \lambda\hbar v_F$

We calculate at zero temperature (i.e. we assume $\mu/k_B \gg T$).

In RPA approximation electron-electron interaction treated self-consistently

$$\chi(q,\omega) \approx \frac{\chi^0(q,\omega)}{1 - v_q\chi^0(q,\omega)} \Rightarrow \varepsilon(q,\omega) \approx 1 - v_q\chi^0(q,\omega)$$

v_q is in-plane Coulomb potential.

Plasmons: C2DES vs 2DES

2DEG

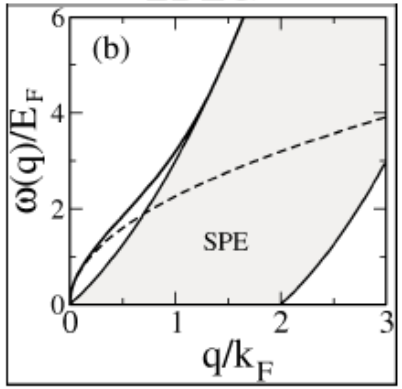

Graphene

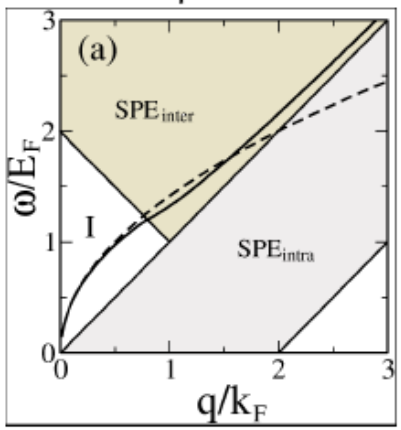

E. Hwang, S. Das Sarma, cond-mat/0610561

- Damping due to interband excitations absent in 2DEG. Stability regime increases proportional to doping μ. For $\mu = T = 0$ plasmons are always unstable, however not at T>0[3]

2DEG

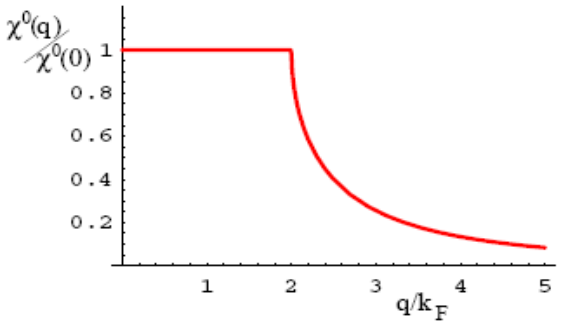

Graphene

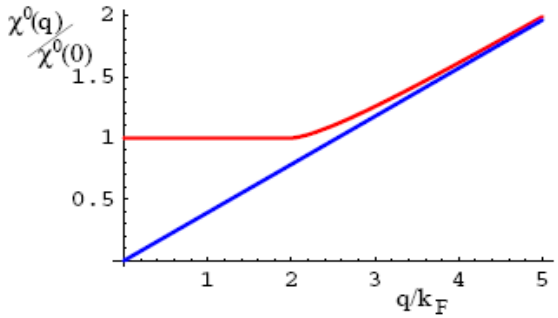

Chiral Linhard Function

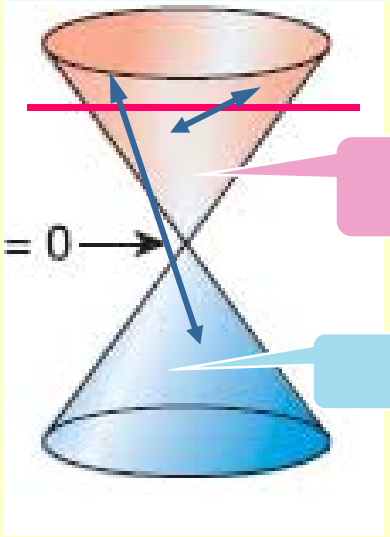

Shung PRB (1986)
Wang PRL **99**, 236802 (2007)
Wunch N J P. *8*, 318 (2006)
Hwang PRB *75*, 205418 (2007)

$\chi^0(q,i\Omega)$

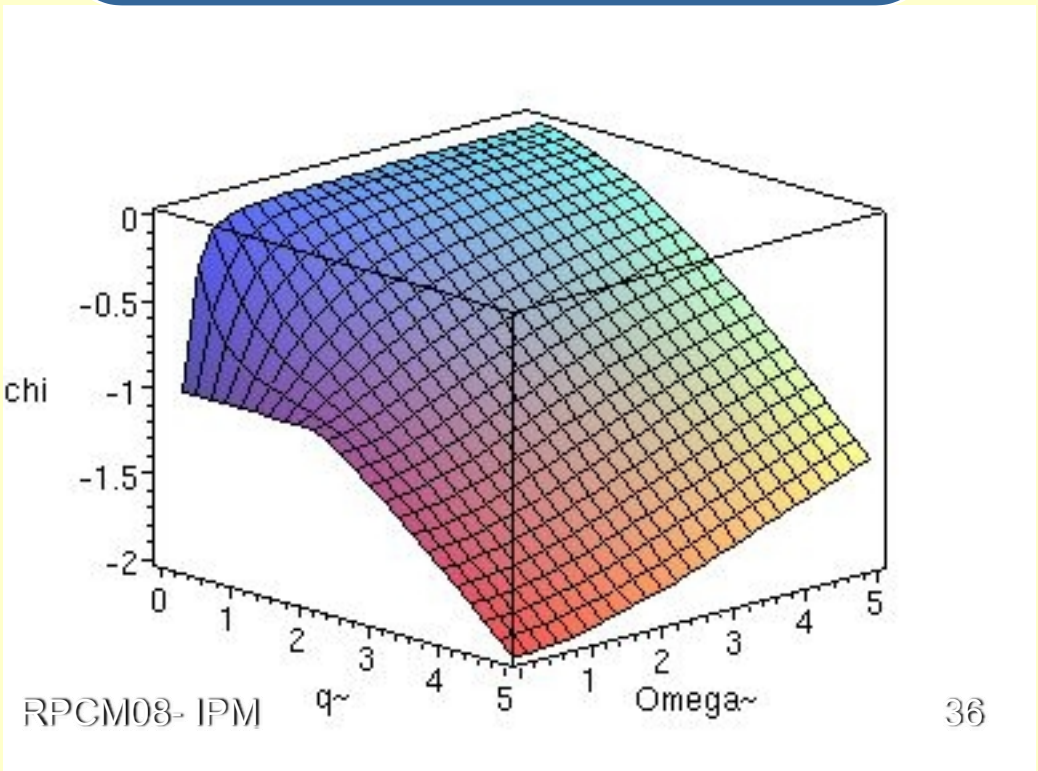

Barlas, Tami, Asgari, Polini

MacDonald PRL**93**, 236601 (2007)

Ground State Energy: RPA

$$
\begin{aligned}
E(1) &= E(0) + E_{\rm x} + \frac{N}{2}\int_0^1 d\lambda \int \frac{d^2\mathbf{q}}{(2\pi)^2}\, v_q \left\{ -\frac{1}{\pi n}\int_0^{+\infty} d\Omega \, \left[\chi^{(\lambda)}_{\rho\rho}(\mathbf{q}, i\Omega) - \chi^{(0)}_{00}(\mathbf{q}, i\Omega, \mu \neq 0) \right] \right\} \\
&= E(0) + E_{\rm x} + E_{\rm c}\,,
\end{aligned}
$$

$$
\varepsilon_{\rm x} = \frac{E_{\rm x}}{N} = \frac{1}{2}\int \frac{d^2\mathbf{q}}{(2\pi)^2}\, v_q \left[-\frac{1}{\pi n}\int_0^{+\infty} d\Omega \, \chi^{(0)}_{00}(\mathbf{q}, i\Omega, \mu \neq 0) - 1 \right]
$$

$$
\chi^{(\lambda)}_{\rho\rho}(\mathbf{q}, i\Omega) \rightarrow \frac{\chi^{(0)}_{00}(\mathbf{q}, i\Omega, \mu \neq 0)}{1 - v_q^{(\lambda)} \chi^{(0)}_{00}(\mathbf{q}, i\Omega, \mu \neq 0)}
$$

$$
\begin{aligned}
\varepsilon_{\rm c}^{\rm RPA} = \frac{E_{\rm c}}{N} &= \frac{1}{2}\int_0^1 d\lambda \int \frac{d^2\mathbf{q}}{(2\pi)^2}\, v_q^2 \left\{ -\frac{1}{\pi n}\int_0^{+\infty} d\Omega \, \frac{\lambda [\chi^{(0)}_{00}(\mathbf{q}, i\Omega, \mu \neq 0)]^2}{1 - \lambda v_q \chi^{(0)}_{00}(\mathbf{q}, i\Omega, \mu \neq 0)} \right\} \\
&= \frac{1}{2\pi n}\int \frac{d^2\mathbf{q}}{(2\pi)^2}\int_0^{+\infty} d\Omega \left\{ v_q \chi^{(0)}_{00}(\mathbf{q}, i\Omega, \mu \neq 0) + \ln\left[1 - v_q \chi^{(0)}_{00}(\mathbf{q}, i\Omega, \mu \neq 0) \right] \right\}
\end{aligned}
$$

$$
\kappa^{-1} = n^2 \frac{\partial^2 (n \delta\varepsilon_{\rm tot})}{\partial n^2}
$$

$$
\delta\varepsilon_{\rm kin}(\zeta) = \frac{2}{3}\varepsilon_{\rm F}\frac{(1+\zeta)^{3/2} + (1-\zeta)^{3/2}}{2}\,.
$$

$$
\left(\frac{1}{\chi_{\rm S}} = \frac{2}{\varepsilon_{\rm F}} \frac{\partial^2 [\delta\varepsilon_{\rm tot}(\zeta)]}{\partial \zeta^2}\bigg|_{\zeta=0} \right.,
$$

Spin Suseptibility

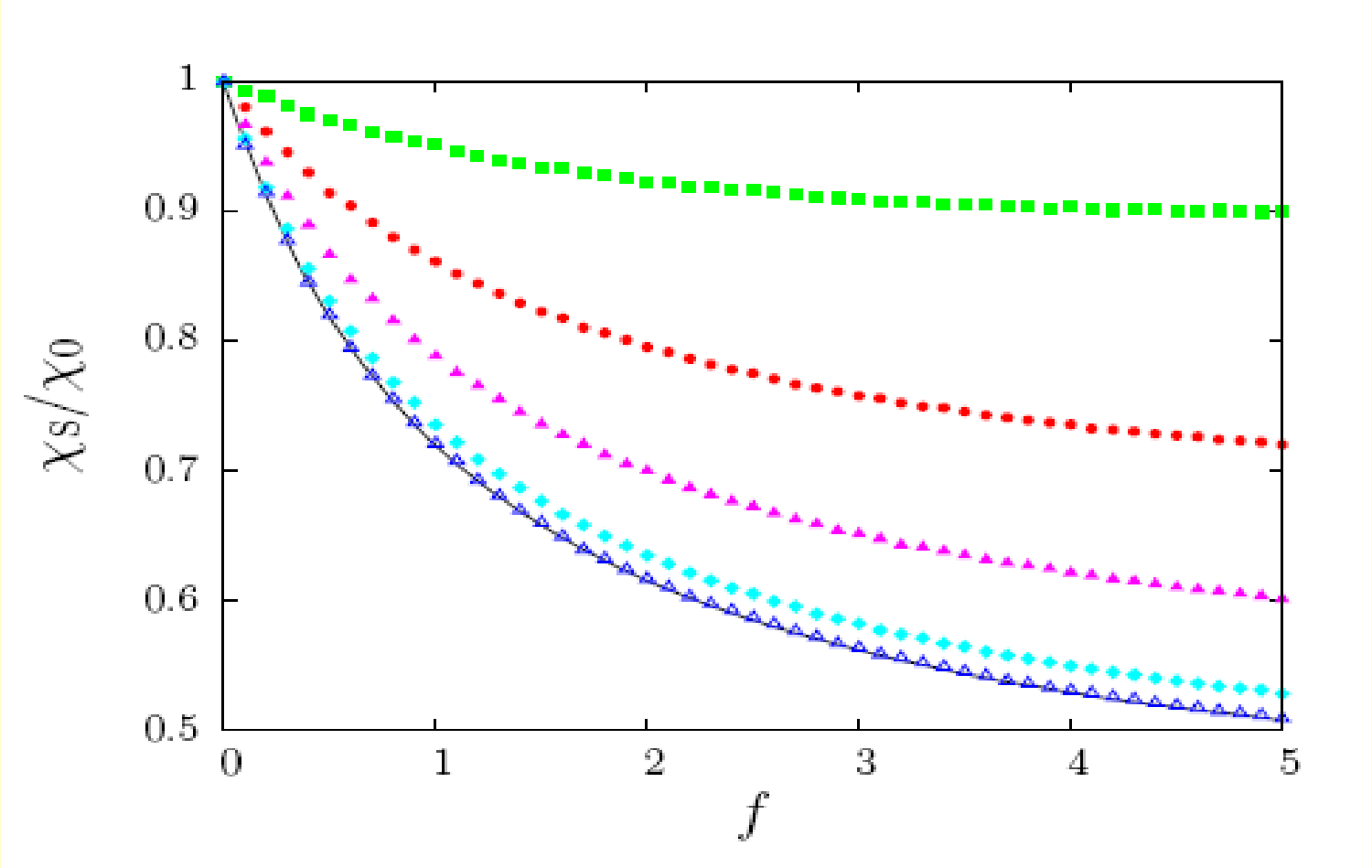

$$f \equiv \nu \frac{2\pi e^2}{\epsilon k_F} = g \frac{e^2}{\epsilon v \hbar}$$

$$\left(\frac{1}{\chi_S} = \frac{2}{\varepsilon_F} \left. \frac{\partial^2 [\delta \varepsilon_{tot}(\zeta)]}{\partial \zeta^2} \right|_{\zeta=0} \right),$$

Barlas, Tami, Asgari, Polini MacDonald PRL **93**, 236601 (2007)

Compressibility

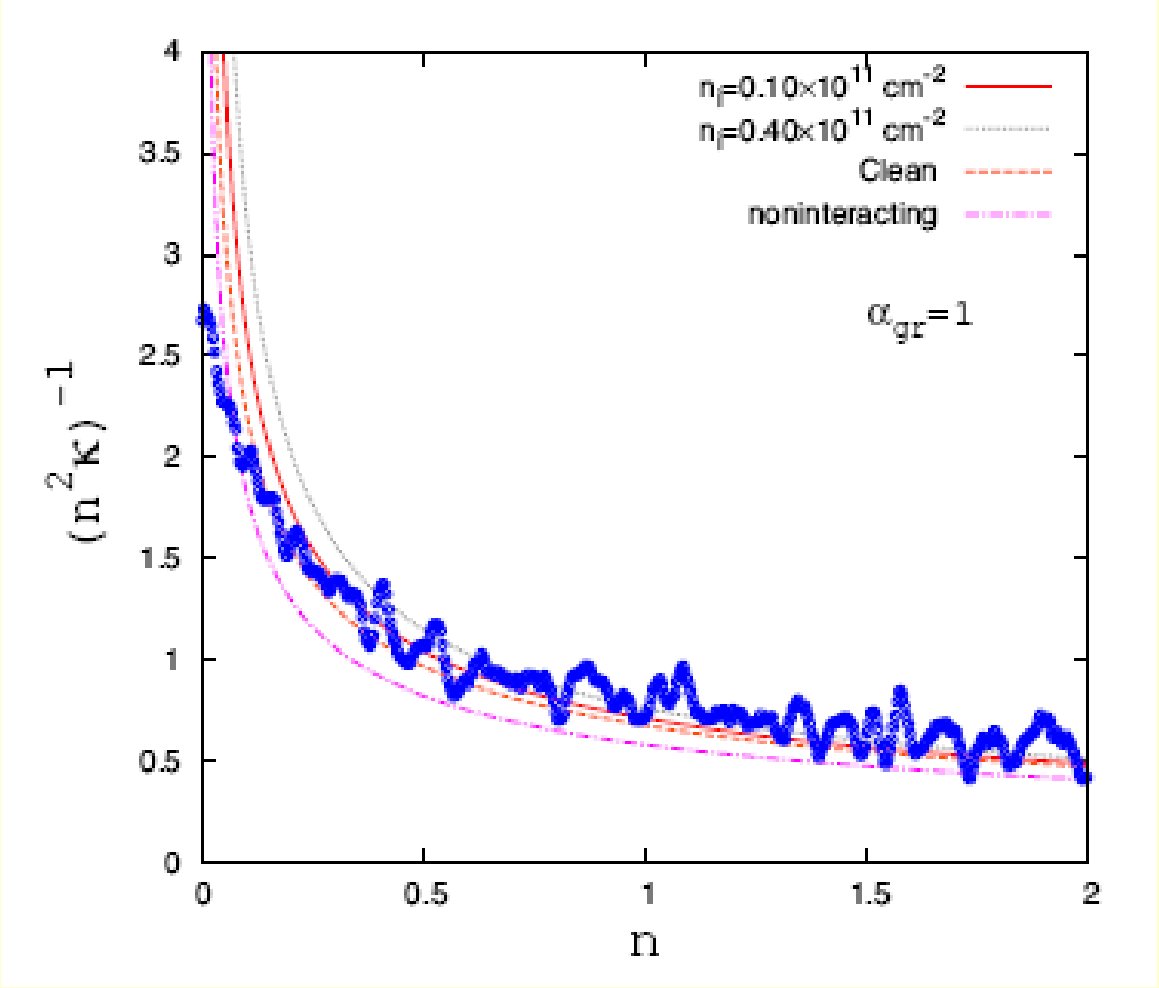

Asgari, *et al* PRB **77**, 125432 (2008)

Self-enery

$$\Im m\Sigma_s^{\rm ret}(\mathbf{k},\omega) = \sum_{s'}\int \frac{d^2\mathbf{q}}{(2\pi)^2} v_q \Im m[\varepsilon^{-1}(\mathbf{q},\omega-\xi_{s'}(\mathbf{k}+\mathbf{q}))]\left[\frac{1+ss'\cos\left(\theta_{\mathbf{k},\mathbf{k}+\mathbf{q}}\right)}{2}\right]$$
$$\times\ [\Theta(\omega-\xi_{s'}(\mathbf{k}+\mathbf{q}))-\Theta(-\xi_{s'}(\mathbf{k}+\mathbf{q}))]\ .$$

$$\Im m[\Sigma_+(0,\omega\to 0)] = -\frac{\sqrt{3}}{8g}\frac{\alpha_{\rm gr}^2}{(1+\alpha_{\rm gr})^2}\omega^2\ .$$

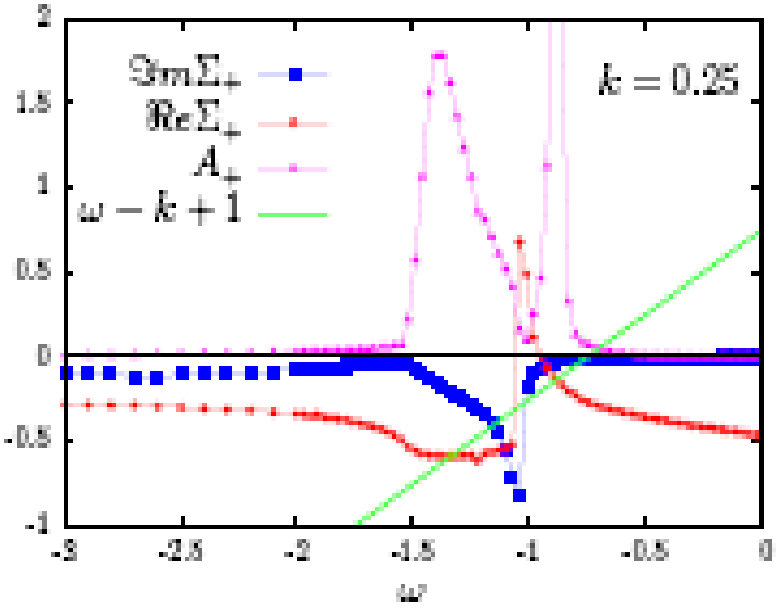

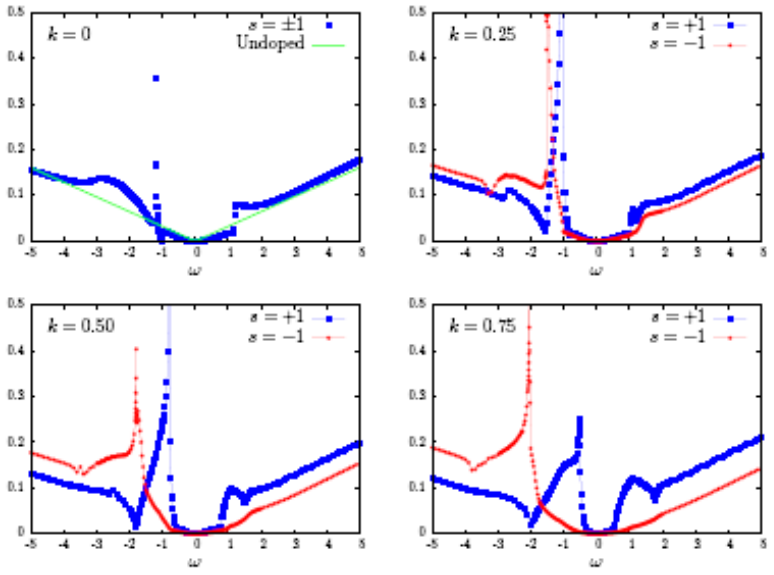

FIG. 3: (Color online) The absolute value $|\Im m[\Sigma_s(k,\omega)]|$ of the imaginary part of the RPA quasiparticle self-energy (in units of $\varepsilon_{\rm F}$) of an n-doped system as a function of energy ω for $k=0, 0.25, 0.50$, and 0.75 and for $\alpha_{\rm gr}=2$.

Polini, Asgari, Barlas Tami, MacDonald PRB **77**, 081411 (R) (2008)

Spectral function: Open Gap!

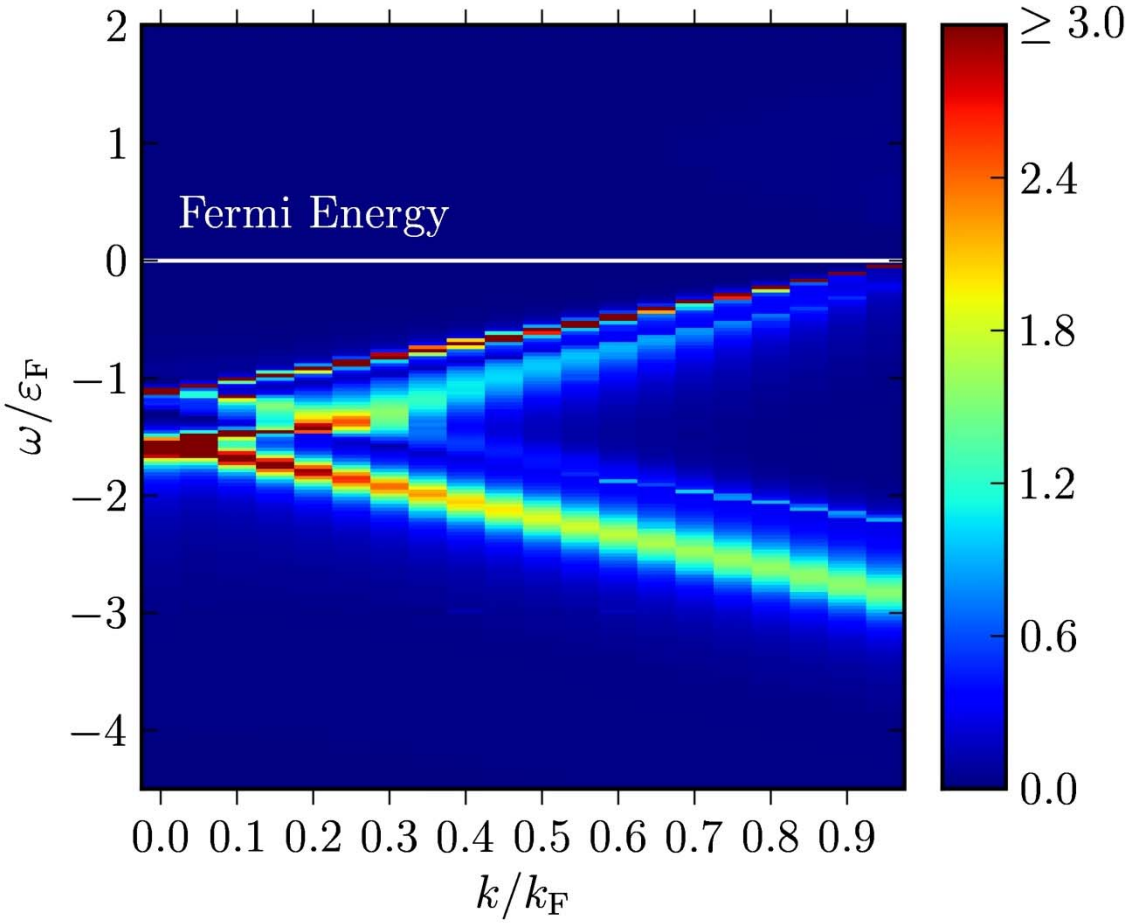

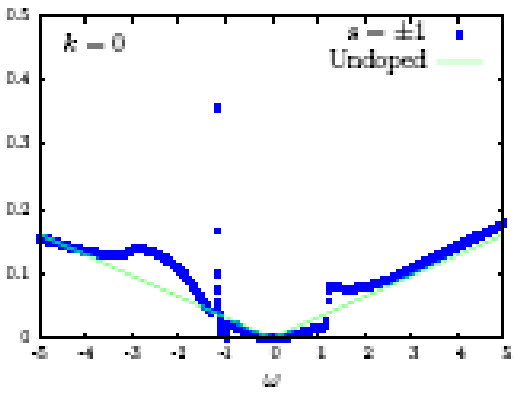

Polini, Asgari, Barlas
Tami, MacDonald
PRB **77**, 081411 (R) (2008)

$$\mathcal{A}_s(\mathbf{k},\omega) = \frac{1}{\pi}\frac{|\Im m\Sigma_s^{\rm ret}(\mathbf{k},\omega)|}{[\omega - \xi_s(\mathbf{k}) - \Re e\Sigma_s^{\rm ret}(\mathbf{k},\omega)]^2 + [\Im m\Sigma_s^{\rm ret}(\mathbf{k},\omega)]^2}\,.$$

e-h Puddles

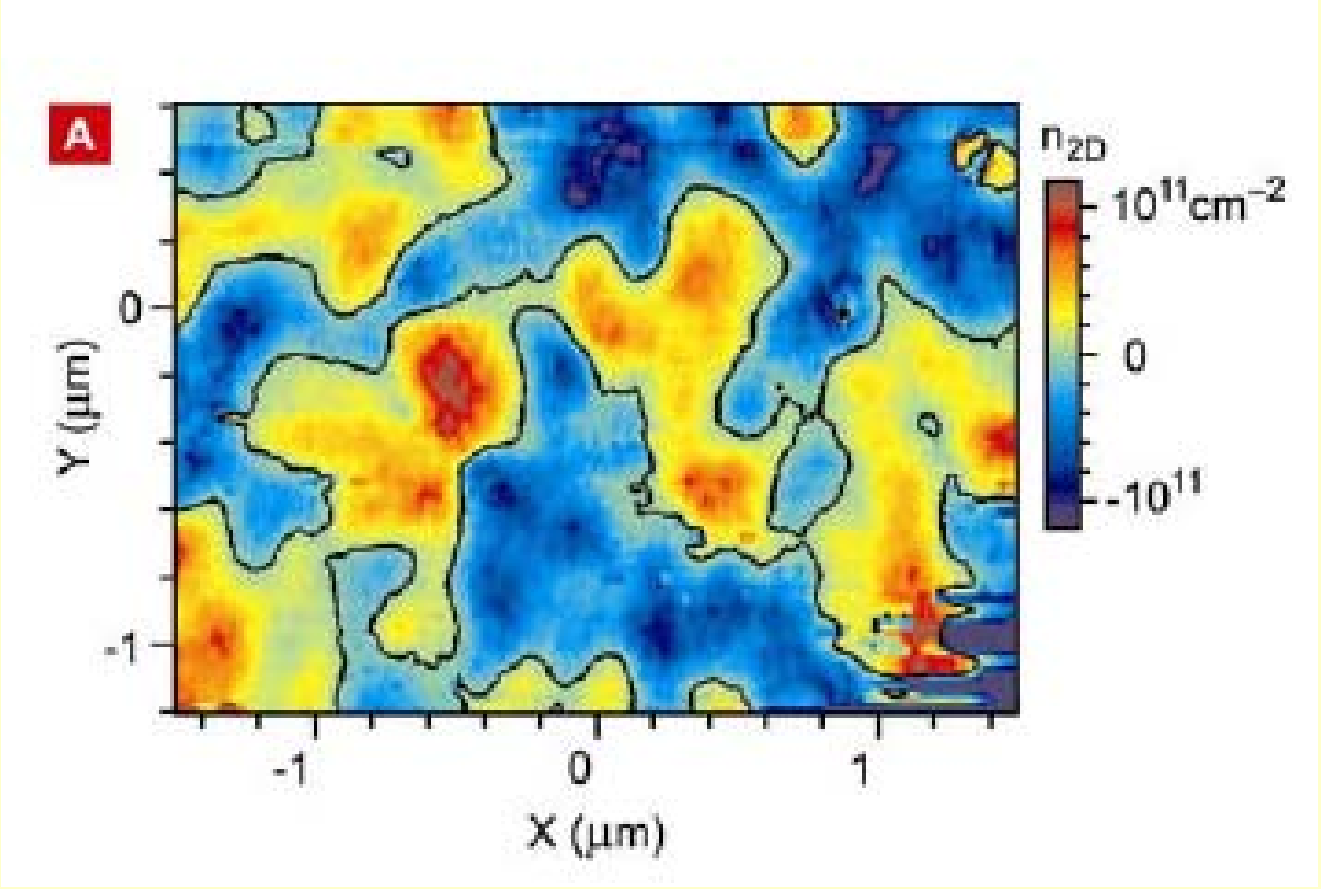

Martin *et al.* Nature Physic **4**, 144 (2007)

XC in Graphene

$$\delta\varepsilon_{\mathbf{x}}(n) = \varepsilon_{\mathbf{F}}\alpha_{\mathbf{gr}}F(\Lambda)$$

$$F(\Lambda) = \frac{1}{6g}\ln(\Lambda) + \frac{a_0}{1 + b_0\ \Lambda^{c_0}}$$

$$\begin{cases} a_0 = 0.0173671 \\ b_0 = 3.6642 \times 10^{-7} \\ c_0 = 1.6784 \end{cases}$$

$$\Lambda(n) = \sqrt{g\eta}\frac{1}{\sqrt{|n|\mathcal{A}_0}}$$

$$\frac{\delta\varepsilon_{\mathbf{c}}^{\mathrm{RPA}}(n)}{\varepsilon_{\mathbf{F}}} = -\frac{\alpha_{\mathbf{gr}}^2}{6g}\xi(\alpha_{\mathbf{gr}})\ln(\Lambda) + \frac{\alpha_{\mathbf{gr}}^2\ a_{\mathbf{c}}(\alpha_{\mathbf{gr}})}{1 + b_{\mathbf{c}}(\alpha_{\mathbf{gr}})\Lambda^{c_{\mathbf{c}}(\alpha_{\mathbf{gr}})}}$$

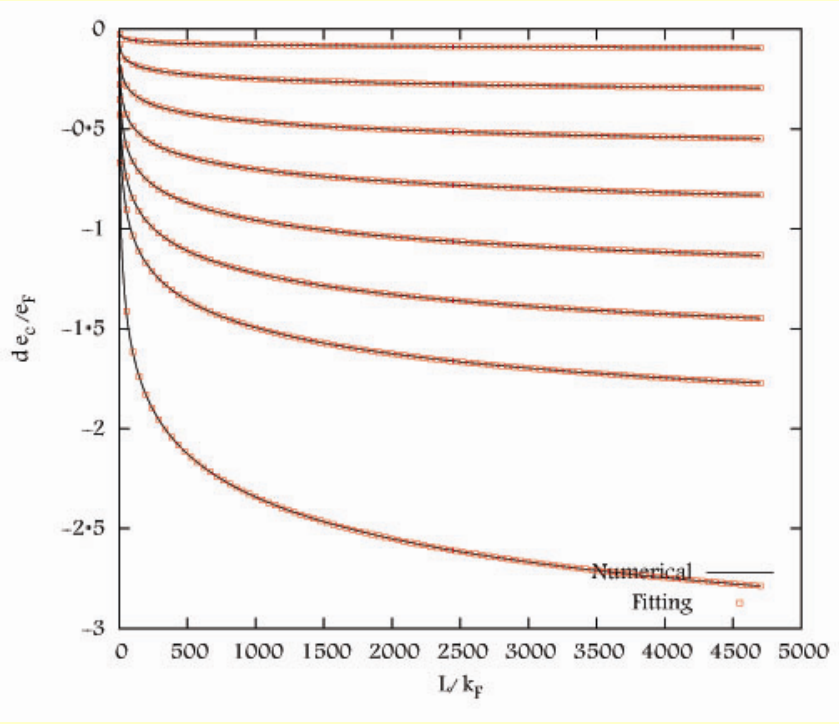

$$\begin{cases} a_{\mathbf{c}}(\alpha_{\mathbf{gr}}) = -1/(63.0963 + 57.351226\ \alpha_{\mathbf{gr}}) \\ b_{\mathbf{c}}(\alpha_{\mathbf{gr}}) = (7.75095 - 0.08371\ \alpha_{\mathbf{gr}}^{1.61167}) \times 10^{-7} \\ c_{\mathbf{c}}(\alpha_{\mathbf{gr}}) = 1.527 + 0.0239\ \alpha_{\mathbf{gr}} - 0.001201\ \alpha_{\mathbf{gr}}^2 \end{cases}$$

$$\xi(\alpha_{\mathbf{gr}}) = \frac{1}{2}\int_0^{+\infty}\frac{dx}{(1+x^2)^2(\sqrt{1+x^2} + \pi\alpha_{\mathbf{gr}}/8)}$$

Polini, Asgari, MacDonald, CM/0803.4150

XC potential in C2DES vs 2DEG

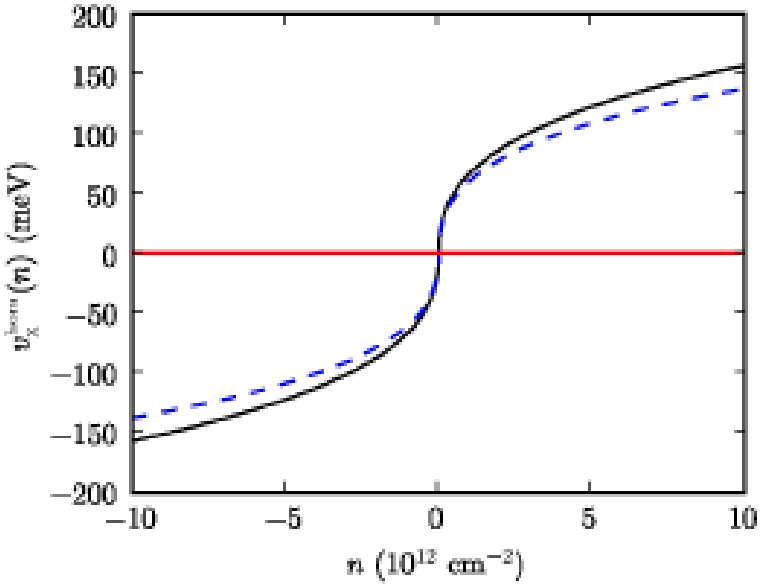

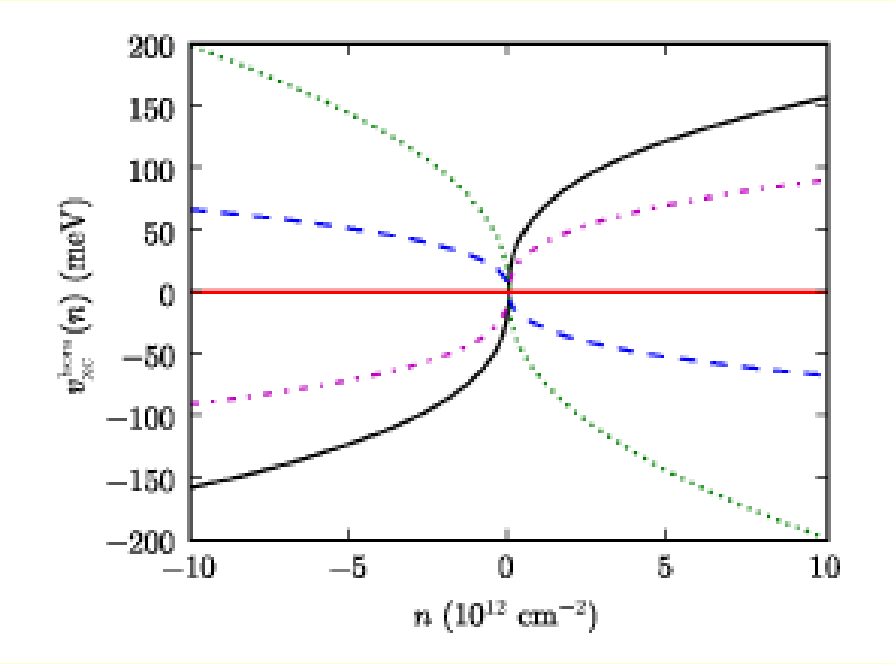

$$v_{\mathrm{x}}^{\mathrm{hom}}(n \to 0) \propto -\mathrm{sgn}(n)\alpha_{\mathrm{gr}}\sqrt{|n|}\ \ln|n|$$

$$v_{\mathrm{c}}^{\mathrm{hom}}(n \to 0) \propto \mathrm{sgn}(n)\alpha_{\mathrm{gr}}^{2}\xi(\alpha_{\mathrm{gr}})\sqrt{|n|}\ \ln|n|$$

DFT in Graphene

$$\Phi_\lambda(\boldsymbol{r}) = (\varphi_\lambda^{(A)}(\boldsymbol{r}), \varphi_\lambda^{(B)}(\boldsymbol{r}))^{\mathrm{T}}$$

$$\left[v\boldsymbol{\sigma}\cdot\boldsymbol{p} + \mathbb{I}_\sigma V_{\mathrm{KS}}(\boldsymbol{r})\right]\Phi_\lambda(\boldsymbol{r}) = \varepsilon_\lambda \Phi_\lambda(\boldsymbol{r})$$

$$\Delta V_{\mathrm{H}}(\boldsymbol{r}) = \int d^2\boldsymbol{r}' \frac{e^2}{\epsilon|\boldsymbol{r}-\boldsymbol{r}'|}\,\delta n(\boldsymbol{r}')$$

$$v_{\mathrm{xc}}^{\mathrm{hom}}(n) = \frac{\partial[n\delta\epsilon_{\mathrm{xc}}(n)]}{\partial n}$$

$$V_{\mathrm{ext}}(\boldsymbol{r}) = -\sum_{i=1}^{N_{\mathrm{imp}}} \frac{Ze^2}{\epsilon\sqrt{|\boldsymbol{r}-\boldsymbol{R}_i|^2 + d^2}}$$

$$\begin{aligned} n(\boldsymbol{r}) &= 4\sum_{\lambda(\mathrm{occ})} \Phi_\lambda^\dagger(\boldsymbol{r})\Phi_\lambda(\boldsymbol{r}) \\ &\equiv 4\sum_{\lambda(\mathrm{occ})} [|\varphi_\lambda^{(A)}(\boldsymbol{r})|^2 + |\varphi_\lambda^{(B)}(\boldsymbol{r})|^2] \end{aligned}$$

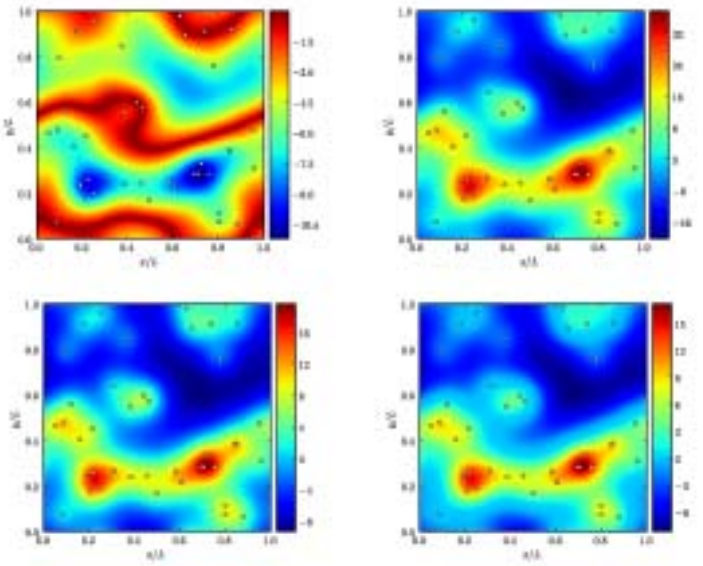

FIG. 2: (Color online) Top left panel: a color plot of the external potential $V_{\mathrm{ext}}(r)$ (in units of $\hbar v/L$) as a function of x/L and y/L. The system parameters are $N_x = N_y = 128$, $k_c = (2\pi/L) \times 10$, $N_{\mathrm{imp}} = 40$, $Z = +1$, $\alpha_{ee} = 0.5$, $\mathcal{Q} = 0$, and $d/L = 0.1$. The small circles represent the positions of the impurities for a particular realization of disorder. Top right panel: a color plot of the corresponding non-interacting ground-state density profile $\delta n(r)$ (in units of $1/L^2$) as a function of x/L and y/L. Bottom left panel: Hartree-only ground-state density profile. Bottom right panel: same as in the bottom left panel but with the addition of the exchange and RPA correlation potential.

Polini, Asgari, MacDonald, CM/0803.4150

Thanks for your attention

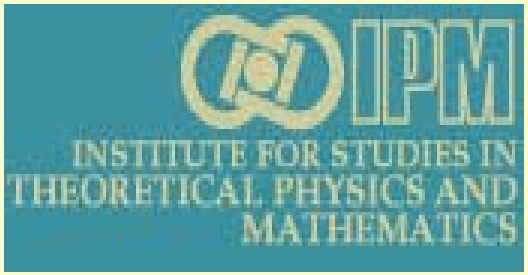

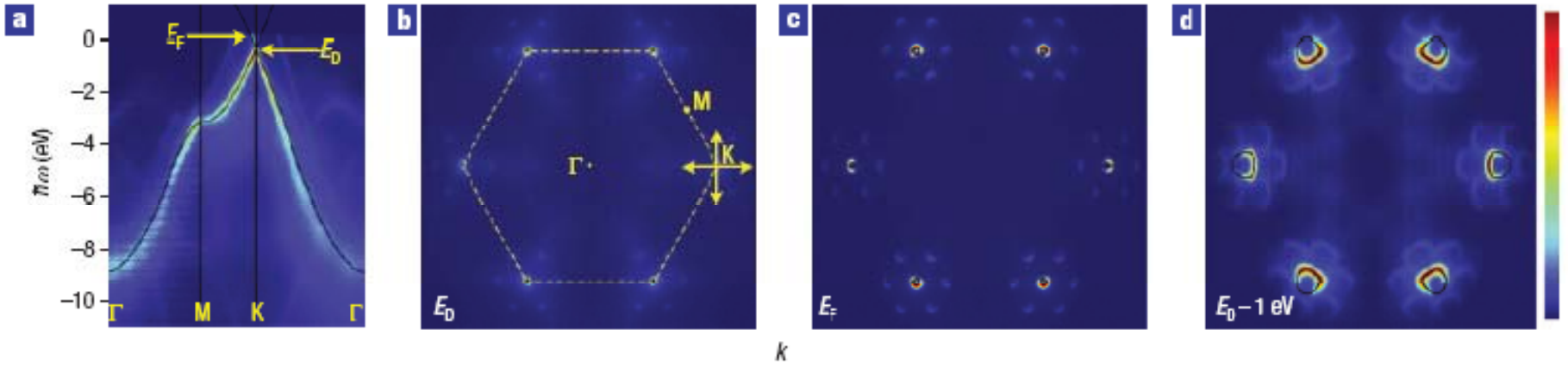

Figure 1 The band structure of graphene. **a**, The experimental energy distribution of states as a function of momentum along principal directions, together with a single-orbital model (solid lines) given by equation (1). **b**, Constant-energy map of the states at binding energy corresponding to E_D together with the Brillouin zone boundary (dashed line). The orthogonal double arrows indicate the two directions over which the data in Fig. 2 were acquired. **c**,**d**, Constant-energy maps at $E_F(=E_D+0.45)$ (**c**) and E_D-1 eV (**d**). The faint replica ba

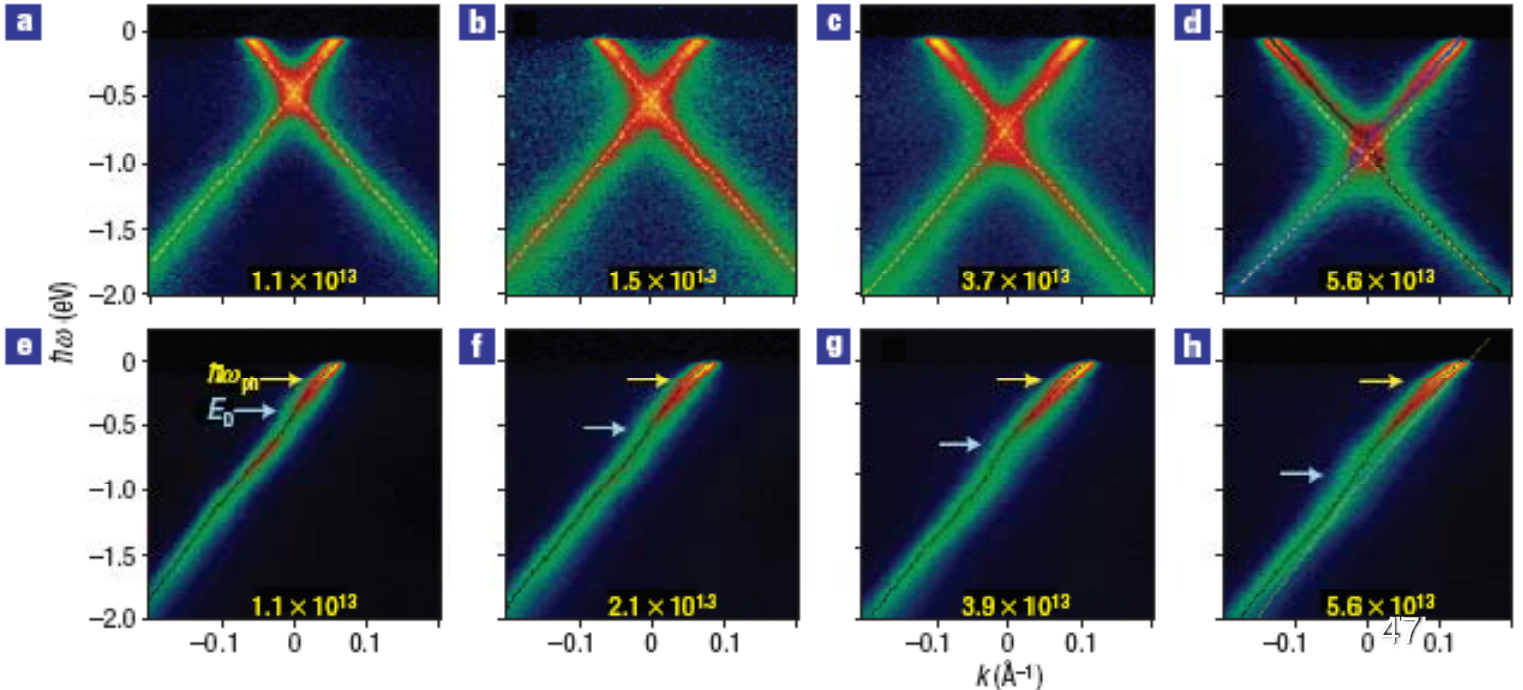

Rotenberg's group, Nature physics **3**, 36 (2006)

Minding the gap in expitaxial graphene

SiC substrate, gap is 0.26 eV

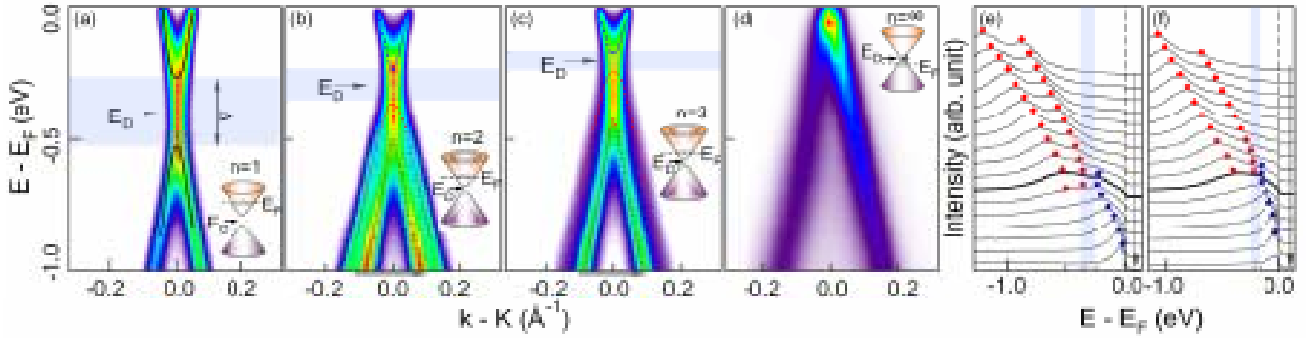

FIG. 2: (a-c) ARPES intensity maps taken near the K point for single layer, bilayer and trilayer graphene samples respectively. Data in panels (b) and (c) are taken along ΓK direction and symmetrized with respect to the K point to remove the strong intensity asymmetry induced by dipole matrix element [11]. The solid lines are dispersions extracted from the EDC peak positions. The dotted lines in panels (b) and (c) are obtained by symmetrizing the extracted dispersions with respect to the K point. The light blue shaded area labels the gap region and the arrow labels E_D. (d) ARPES intensity map taken near the H ($k_z=\pi/c$) point of graphite, where the dispersion resembles graphene. (e, f) EDCs taken from the raw data (without symmetrization) for momentum regions labeled by the arrows in the bottom of panels (b) and (c). Red and blue symbols label peak positions in the EDCs.

Zhou *et al.* Nature Material **6**, 770(2007)

Single impurity

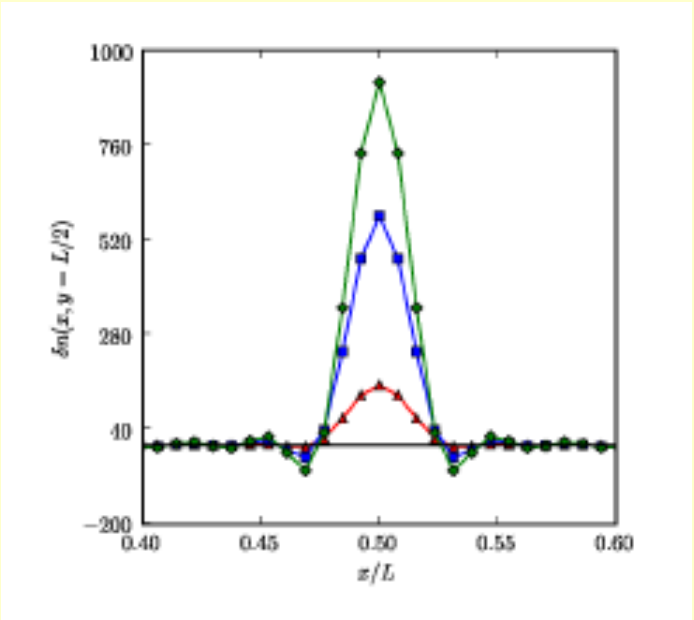

Pseudospin, Helicity and Chirality

Helicity (particle physics)

From Wikipedia, the free encyclopedia

In particle physics, **helicity** is the projection of the angular momentum to the direction of motion:

Because the angular momentum with respect to an axis has discrete values, helicity is discrete, too. For spin-1/2 particles such as the electron, the helicity can either be positive - the particle is then "right-handed" - or negative - the particle is then "left-handed".

For massless (or extremely light) spin-1/2 particles, helicity is equivalent to the operator of chirality multiplied by h/2

$$\hat{H} = \hbar v_F \begin{pmatrix} 0 & k_x - ik_y \\ k_x + ik_y & 0 \end{pmatrix} = \hbar v_F \sigma \cdot \mathbf{k},$$